Doctoral Thesis

On Performance Modeling of 3D Mobile Ad Hoc Networks

by

Wu Wang

Graduate School of Systems Information Science

Future University Hakodate

March 2018

Abstract

Three-dimensional mobile ad hoc networks (3D MANETs) are a class of peer-to-peer networks, where nodes moving in three-dimensional space communicate with each other via wireless link without any pre-existing infrastructure and central management. As 3D MANETs can be easily deployed and flexibly reconfigured, they are used in many fields, such as (1) modern warfare, aircrafts in the sky, troops on the land, fleets on the sea, communicate with each other for cooperative combat, (2) ocean surveillance, underwater vehicles communicate with each other for data collection and transmission, (3) disaster monitoring, unmanned aerial vehicles communicate with each other for data collection and transmission.

However, there is still a long way to go before 3D MANETs could be widely commercialized and implemented. The very roadblock that has been stunting the application of 3D MANETs is the lack of a general network information theory, which is expected to establish a thorough understanding on the fundamental performances in such networks, like the delivery probability, delivery delay, throughput capacity, etc. The available works on this line mainly focus on two-dimensional network scenario, which cannot tell us about the fundamental performances in 3D MANETs. Towards such a target in 3D MANETs, we develop theoretical frameworks to analytically study the MANET delivery probability, delay and the throughput capacity performances in this thesis. Specifically, we focus on an important class of 3D MANETs—the two-hop relay 3D MANETs, i.e., the MANETs adopting the popular and efficient two-hop relay algorithms for packet routing.

Firstly, we study packet delivery probability in 3D MANETs. We develop a Markov chain theoretical framework to depict packet delivery process under two-hop relay algorithm with packet redundancy. With the help of the theoretical framework, the analytical expression was derived for packet delivery probability. We further present extensive simulation and numerical results to validate our theoretical framework and to show our findings. We also attempt to simulate the packet delivery probability over the broadcast channel mode. When a node gets a transmission opportunity, it broadcasts the copies of the packet to the nodes which locate in the same cell or its 26 adjacent cells. The number of the broadcast is set to f for each packet. The simulation results show that the delivery probability of using broadcast is higher than using unicast. Although the simulation results show that the delivery probability performance under broadcast is better than that under unicast. This thesis does not adopt the broadcast traffic pattern. This is because under such a traffic pattern, the number of relay nodes carrying the packet is unknown, which makes it more difficult to develop a Markov chain to analytically study the packet delivery performance.

Secondly, we study the packet delivery delay performance in 3D MANETs. A Markov chain theoretical frame is developed to depict packet delivery process under two-hop relay algorithm with packet redundancy. Under the Markov chain theoretical framework, the analytical expression was derived for mean packet delivery delay. Besides that, the corresponding relative standard deviation was further derived. We provide simulation results to validate the theoretical models on the packet delivery

delay and corresponding relative standard deviation not only under independent and identically distributed (i.i.d.) mobility model, but also under the random walk and random waypoint mobility models. Extensive simulation and numerical results with different parameters are further provided to do performance analysis and show the packet delivery performance in 3D MANET is different from that in 2D MANET.

Thirdly, we study the throughput capacity in 3D MANETs. We first construct two absorbing Markov chain theoretical frameworks to depict the packet distributing process at source and the packet receiving process at destination. Based on these two Markov chain theoretical frameworks, an analytical expression for the throughput capacity is further derived. We provide extensive simulation and numerical results to validate our theoretical models and to show our findings.

Finally, we introduce our future works. In this thesis, we adopt unicast for packet dispatching, one interesting future direction is to further explore the performance of 3D MANETs under a more efficient packet dispatching way, e.g. broadcast. We developed Markov chain-based theoretical frameworks to explore packet delivery performance in cell-partitioned 3D MANETs, it will be an interesting direction to study how to evaluate the performance under our theoretical frameworks in other network scenarios, such as delay tolerant networks (DTNs) and ALOHA networks. We focus on two-hop relay 3D MANETs, another interesting direction is to further extend the developed theoretical models to analyze packet delivery performance in multi-hop relay 3D MANETs. It is also interesting to explore the network performance with the consideration of constraints of nodes buffer size and packet loss in our future research.

Acknowledgments

I would like to express my deepest gratitude to all those who gave me the opportunity to complete this thesis. First and foremost, I am deeply indebted, grateful to my supervisor, Professor Xiaohong Jiang for giving me copious amounts of insightful guidance, constant support, and expertise on every subject that arose throughout all these years. He is more than a supervisor and a teacher but a role model and a friend. Working with him is proven to be an enjoyable and rewarding experience. I would also like to give my special thanks to Dr. Bin Yang for giving me a lot of help in my academic research. This thesis would not have been possible without their guidance.

I would like to acknowledge my thesis committee members, Professor Yuichi Fujino, Professor Hiroshi Inamura and Professor Masaaki Wada, for their interests and for their constructive comments that help to improve this thesis.

I would like to give my sincere thanks to Professor Osamu Takahashi for his generous support. I am also very grateful to all the people I have interacted with at Future University Hakodate, specifically everyone affiliated with Jiang's Laboratory. My graduate study at the Future University Hakodate has been a really rewarding experience.

This work is dedicated to my family, whose love and unconditional support provide a constant inspiration in my life. In particular, I would like to thank my wife for her understanding, encouragement, and support in these years.

THIS PAGE INTENTIONALLY LEFT BLANK

Contents

List of Figures

Chapter 1

Introduction

In this chapter, we first introduce the background of mobile ad hoc networks (MANETs) [1]. We then describe our motivations of this thesis.

1.1 Background

With the development of science and technology, especially the rapid development of smart phones, wireless networks have become an indispensable part of our daily lives. We access Internet via wireless networks to complete the most affair in our studying, live and entertainment, such as booking hotel,calling taxi, shopping. However, these wireless networks rely heavily on centralized control such as cellular network, the terminal devices communication need relaying from base stations. Once the base stations are destroyed by nature disasters or malicious attacks, the terminal devices will not work any more. Motivated by this, many researchers from both academia and industry have been making efforts to develop a novel class of wireless networks named mobile ad hoc networks(MANETs). In such networks, terminal devices can reconfigure by themselves, communication with each other via wireless channel without helps of central base station.

The followings are the MANETs features which distinguish from traditional wireless networks. Firstly, they can be easily deployed, especially in those geographically tough areas, since they are built without the support of infrastructure or base sta-

tion. Secondly, they can be flexibly reconfigured, when any node is unavailable due to power fails or other reasons, the remainder nodes which in the communication range can communication with each other. It commonly happens due to the mobility of nodes. Finally, they can provide low-cost Internet service for these users residing in remote areas.

Three-dimensional mobile ad hoc networks (3D MANETs) are an important class of MANETs, where nodes moving freely in three-dimensional space communicate with each other via wireless link without any pre-existing infrastructure and central management. Airborne ad hoc networks (AANETs), underwater wireless sensor networks (UWSNs) and underground sensor networks(UGSNs) are three good examples for such networks, they are shown in Figure 1-1, Figure 1-2 and Figure 1-3, respectively.

AANETs can be used to businesses, private internet users, government agencies and military. For instance, at modern war, an airborne network might enable military planes to communicate with each other without a fixed communications infrastructure. Such networks are also useful for civilian aviation to allow civilian planes to continually monitor each other's positions and flight paths.

UWSNs can find applications in oceanographic data collection, pollution monitoring, offshore exploration, disaster prevention. 3D UWSNs are used to detect and observe phenomena that can not be adequately observed by means of ocean bottom sensor nodes (2D sensor networks), i.e., to perform cooperative sampling of the 3D ocean environment. In 3D UWSNs, sensor nodes deploy at different depths to enable the exploration of natural undersea resources and gathering of scientific data in collaborative monitoring missions.

Underground sensor networks(UGSNs) [2] can be used to monitor a variety of conditions, such as soil properties for agricultural applications, integrity of below ground infrastructures for plumbing, or toxic substances for environmental monitoring. For example, agriculture can use underground sensors to monitor soil conditions such as water and mineral content [3]. Wireless sensors can also be used to monitor the underground tunnels in coal mines as shown in Figure 1-3. These tunnels are usually long and narrow and distributed in 3D environment, with lengths of tens of kilome-

ters and widths of several meters. A full-scale monitoring of the tunnel environment (including the amount of gas, water, and dust) has been a crucial task to ensure safe working conditions in coal mines industria.

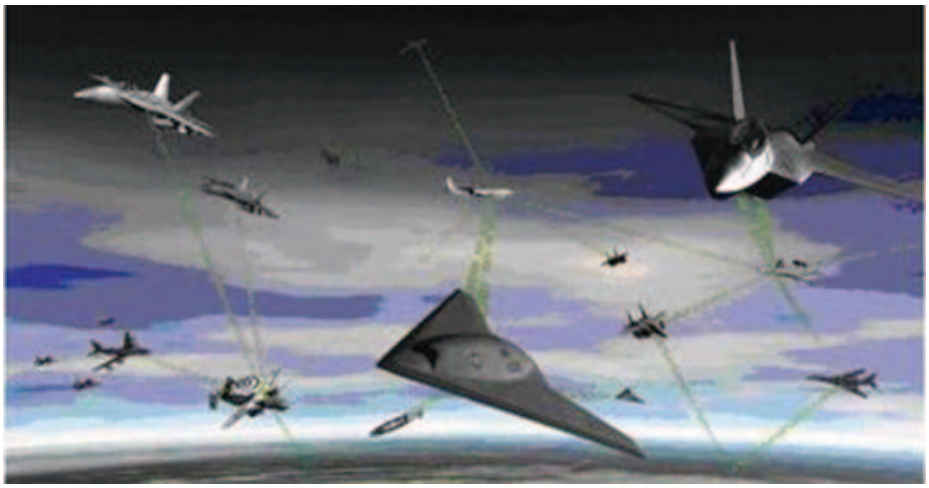

Figure 1-1: An example of airborne ad hoc networks

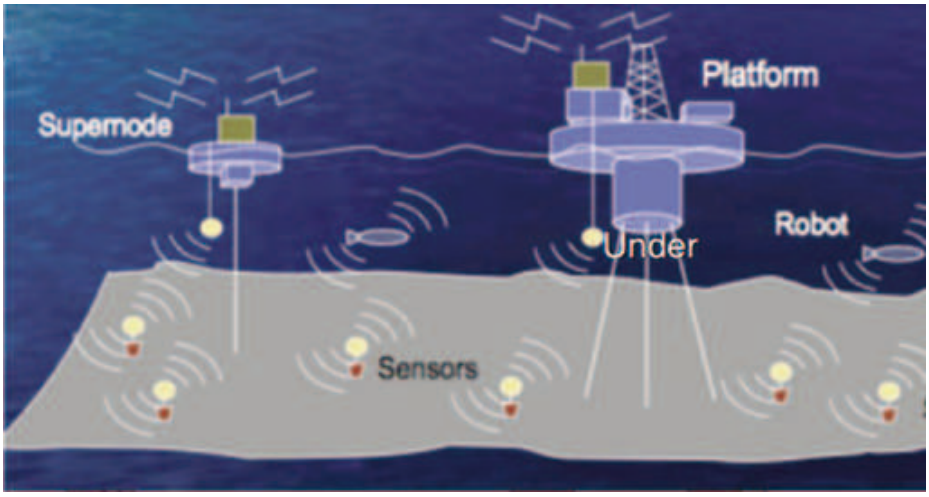

Figure 1-2: An example of underwater wireless sensor networks

1.2 Motivations

Since MANET Group was established by IETF in 1997, extensive studies have been dedicated toward a deeper understanding of the fundamental MANET performance, such as delivery delay [4–14] and throughput capacity [1, 15–23]. Delivery delay is the

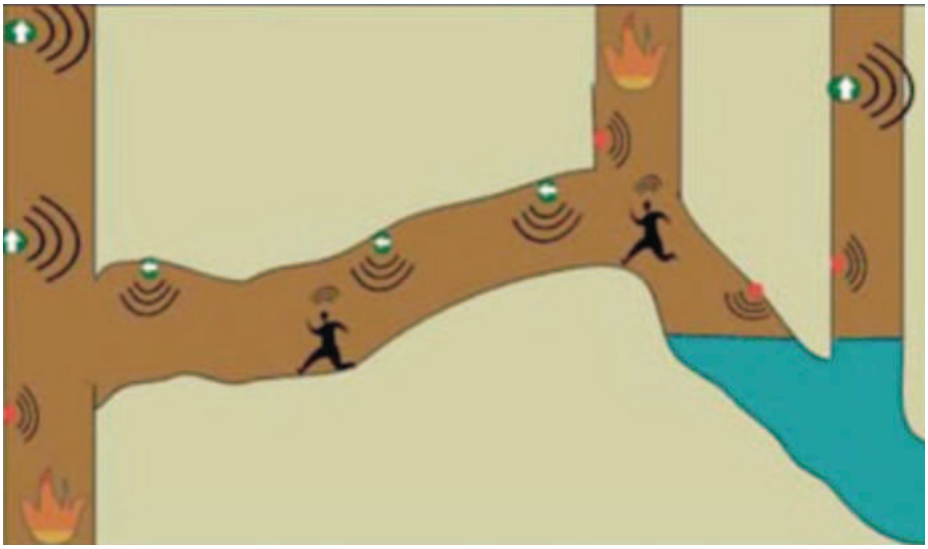

Figure 1-3: An example of underground sensor networks

time duration between the source node starts to deliver the packet and the destination node receives the packet. Throughput capacity is defined as the maximum packet input rate that the considered MANET can stably support under a given routing algorithm. The performance studies of these available works contribute to the design, development and commercialization for MANETs.

However, the above works mainly focus on the performance study in 2D MANETs. In fact, recent interest hints at the strong need to design 3D MANETs. Unfortunately, the design of 3D MANETs is surprisingly more difficult than the design in 2D MANETs. Many properties of the network require additional computational complexity, and many problems can not be solved by extensions or generalizations of 2D methods. For instance, in 2D MANETs, all nodes are distributed in a two dimensional plane, base on the assumption that nodes are deployed on earth surface and where the height of the network is smaller than transmission radius of a node. However, such 2D assumption may no longer be valid if the nodes are distributed over a 3D space, the difference in the third dimension is too large to be ignored. In addition, as introduced earlier, besides large delay, low bandwidth, high error rate and harsh environments, there are many characteristic features in 3D MANETs. For example, in AANETs, nodes move in a high speed, introducing shorter transmission time. In

UWSNs, underwater sensor nodes may move with water, introducing passive mobility. Which are stunting 3D MANETs applications and commercialization. Thus, a thoroughly understanding of the fundamental performance of 3D MANETs is of great importance for their future applications.

1.3 Thesis Outline

In this thesis, the overall aim is to provide a comprehensive study on the fundamental delivery probability, delivery delay and throughput capacity performance in 3D MANETs. The main contents of this thesis are summarized as follows:

Chapter 2 Related works. This chapter presents the previous works related to our study in this thesis.

Chapter 3 Preliminaries. This chapter introduces system models and transmission scheduling scheme involved in our study, which include these issues: the network model, the node mobility model, the communication model and the transmission-set based transmission scheduling scheme.

Chapter 4 Packet Delivery Probability Study in 3D MANETs. In this chapter, we investigate packet delivery probability under two-hop relay algorithm with packet redundancy. First, we develop a Markov chain theoretical framework to characterize packet delivery process. With the help of the model, the analytical expression was derived for packet delivery probability. Finally, we present extensive numerical results to demonstrate the accuracy of packet delivery probability analysis and show our findings.

Chapter 5 Packet Delivery Delay Study in 3D MANETs. This chapter studies the packet delivery delay in 3D MANETs. With the help of the theoretical framework, we derive an analytical expression for the mean packet delivery delay. Besides that, we also derive corresponding relative standard deviation as well. We provide simulation and numerical results to validate the theoretical models on the packet delivery delay and corresponding relative standard deviation not only under independent and identically distributed (i.i.d.) mobility model, but also under the

random walk and random waypoint mobility models. Simulation and numerical results are further provided to do performance analysis and show the packet delivery performance in 3D MANET is different from that in 2D MANET.

Chapter 6 Throughput Capacity Study in 3D MANETs. In this chapter, we study the throughput capacity of 3D MANETs, two Markov chains are established, one is used to analyze the packet deliver process at source node (transmitter), the other is used to analyze the packet receive process at destination node (receiver). By exploring the service time at source node and the service time at destination node, we derive the analytical expression for throughput capacity. Finally, we provide extensive numerical results to demonstrate the Markov chain theoretical framework and show our findings.

Chapter 7 Conclusion. This chapter concludes the thesis and discusses the interesting future research topics.

Chapter 2

Related Works

In this chapter, we present a survey of related works on 3D MANET.

2.1 Studies of Packet Delivery Probability

By now, a lot of research activities have been conducted to study the delivery probability in MANETs. Panagakis *et al.* in [24] analytically derived the packet delivery probability of two-hop relay under a given time limit by approximating the cumulative distributed function (CDF) of packet delivery delay. In this work they assumed that for any node pair the packet can be successfully transmitted whenever they meet each other. Whitbeck *et al.* in [25] explored the impact of packet size on the packet delivery probability. They treated the intermittently connected mobile networks (ICMNs) as edge-Markovian graphs, where each edge is considered independent and has the same transition probability. Later, Krifa *et al.* in [26] proposed a practical and efficient joint scheduling and drop policy that can optimize the delivery probability performance of epidemic routing. More recently, the optimization issue of packet delivery probability under specific energy constraints and packet lifetime requirement has also been intensively addressed in the context of delay tolerant networks (DTNs) [27–30], in which the two-hop relay was adopted for packet routing and a wireless link becomes available whenever two nodes encounter.

Further notice that available works commonly adopt packet redundancy technique

to enhance delivery performance in the challenging MANET environment, in which the source node generates copies for every packet waiting for dispatching, a node receiving a packet may forward it or carry it for long periods of time, and a relay node may keep copies for multiple source-destination pairs. Such combination of packet redundancy and long-term storage cause a severe burden on the mobile nodes which are usually not only power-constrained but also buffer-limited. The remnant copies must somehow be removed. J. Liu *et al.* in [31] adopted a mechanism based on packet sequence number for supposed algorithm. For the tagged transmission flow, the source node S labels each packet P waiting at the send-queue with a *send number* $SN(P)$, such that a packet can be efficiently retrieved from the queue buffers of its source node or relay node(s) using its send number. Similarly, the destination node D also maintains a *request number* $RN(D)$ which indicates the send number of the currently request packet, such that each packet is received in order at the node D. When destination node receives a packet, the copied of this packet can be removed from network buffer since every packet was labeled.

Lifetime associated with a packet is another method to drop redundant packets in network. This method can reduce the network resource consumption in terms of buffer occupation and power consumption while simultaneously satisfy the specified delivery performance requirement.Obviously, it is of more interest for network designers to know the corresponding delivery probability under any given packet lifetime (or permitted delivery delay). Al Hanbali *et al.* in [32] evaluated the main performance metrics of the multicopy two-hop relay (MTR) protocol under the assumption that packets in relay nodes have a limited lifetime.

Wei *et al.* in [33] utilized small-world properties and the time-to-live (TTL, i.e. the packet lifetime) to explore the packet delivery cost, delivery delay and delivery ratio (probability). The delivery ratio was defined as: the ratio between the number of packets that are successfully delivered to their destination nodes within their lifetime to the total number of packets generated.

2.2 Studies of Packet Delivery Delay

There have been many research efforts in the literature to study the packet delivery delay performance in MANETs. Moraes *et al.* in [34] proposed a multiuser diversity strategy for packet relaying in mobile ad-hoc network, which permits more than one-copy of a packet being received by relay nodes, thus allowing to decrease the delay on such networks for a fixed number of total nodes. The bound of delivery delay was also provided in this work.

The packet delivery delay performance in two-hop relay MANETs was studied in [35–37], where [35] considers random walk mobility model, [36] considers restricted mobility model, and [37] considers Brownian mobility model. Later, the packet delivery delay performance was explored in two-hop relay MANETs under discrete random direction model and hybrid random walk model in [38], where the network area is evenly divided into multiple equal-sized cells.

Recently, a lot of research efforts have been devoted to the study of packet delivery delay by adopting packet redundancy technique in DTNs (delay tolerant networks), a special class of sparse MANETs where inference among transmissions can be neglected. Spyropoulos *et al.* in [39] proposed a single period routing algorithm (called spray and wait) for the study of delay performance in DTNs, and Bulut *et al.* in [12] extended the algorithm in [39] and further proposed a more general multi-period spraying algorithm in DTNs. Panagakis *et al.* [11] developed a theoretical framework for delay modeling in DTNs with packet redundancy. Miao *et al.* in [40] proposed an adaptive multi-step routing protocol for DTNs, the protocol reasons on the remaining time-to-live of the packet in order to allocate the minimum number of copies necessary to achieve a given delivery probability. By dynamically allocating packet copies in order to strike a balance between the delay and cost of packet delivery, the proposed protocol has a higher delivery ratio and a lower delivery cost.

It is notable that the above work focuses on the study of order sense scaling laws on packet delivery delay in MANETs. Although the order sense results are helpful for us to understand the growth rate of packet delivery delay with network size, they

tell us little about the exact packet delivery delay. In practice, however, such exact packet delivery delay is of great interest for network designers. Some work is available on the exact packet delivery delay study in MANETs. By establishing an ordinary differential equation, an analytical expression was derived for the packet delivery delay in MANETs [41]. Based on an ordinary differential equation, the exact packet delivery delay and its variants were further studied under epidemic routing in [42]. Later, the exact packet delivery delay was examined in two-hop relay MANETs [43].

2.3 Studies of Throughput Capacity

Throughput capacity is defined as the maximum packet input rate that the considered MANET can stably support under a given routing algorithm.

To study the important yet challenging research problem on throughput capacity, a lot of efforts have been conducted to investigate this issue in two-dimensional MANETs (2D MANETs). The work [15] showed that the per node throughput capacity scales as $\Theta(1/\sqrt{nlogn})$ in wireless ad hoc network without node mobility, where n is the number of nodes in the network.[1] The result suggests that the per node throughput capacity diminishes with increase of n. Some works gave the similar results that the per node throughput capacity tends to 0 as n goes to infinity in the network [18–20]. Later, taking the full advantage of node mobility as an efficient method was introduced in wireless ad hoc networks such as the seminal work [45], where Grossglauser and Tse investigated the throughput capacity of MANETs and showed that the per node throughput capacity can achieve $\Theta(1)$ under identically distributed (i.i.d.) mobility model. Subsequently, researchers showed that the per node throughput capacity could achieve $\Theta(1)$ under various mobility models, such as the Brownian mobility model [46], the restricted mobility model [47] and the random walk model [48]. In addition, there also exist some works that explored the trade-off between throughput capacity and delay in MANETs [21–23].

[1]Recall the following notation [44]: $f(n) = \Theta(g(n))$ means that $f(n) = O(g(n))$ and $g(n) = O(f(n))$, where $f(n) = O(g(n))$ means that there exists a constant c and integer N such that $f(n) \leq cg(n)$ for $n > N$.

The aforementioned researches mainly concern the order sense throughput capacity in the networks. The order sense results contribute to finding how throughput capacity varies with increase of network size n, however, these results cannot explain the exact achievable per node throughput. Actually, such exact throughput capacity will greatly facilitate the practical design and optimization for MANETs. To this end, some initial work has been conducted on the study of the exact throughput capacity. Neely *et al.* [10, 49] derived the exact throughput capacity of cell-partitioned MANETs under Markovian mobility model. Gao *et al.* [50] later extended the above work to that with a group-based scheduling scheme and proved the exact throughput capacity by adopting Lyapunov drift technique. Also, Liu *et al.* [51] investigated the exact throughput capacity under a two-hop relay routing with packet redundancy in MANETs.

Study of exact throughput capacity under the three-dimensional environment, to the best of my knowledge, still remains unexplored. Piyush and P.R. Kumar in [52] show that the capacity achieve under a protocol model of non-interference, in a random 3D network of n nodes randomly located in a sphere, with each node capable of transmitting at W bis/sec and using a common range, the throughput that each node can obtain for a randomly chosen destination is $\Theta(\frac{W}{(nlog^2n)^{\frac{1}{3}}})$ bits/sec. Even under optimal choices for node location, traffic patterns, and origin-destination pairs, and optimal operation by choosing transmission schedules, ranges and routes, each node cannot obtain a throughput of more than $\Theta(\frac{W}{n^{\frac{1}{3}}})$ bits/sec.

Later, some initial works have been dedicated to exploring the performance of 3D MANETs. Pan Li *et al.* in [53] investigated the throughput capacity of both 3D regular ad hoc network and 3D nonhomogeneous ad hoc network, by employing a generalized physical model, and gave lower and upper bounds in both types of network in a broad power propagation regime. It is notable that although the above mentioned works gave the approximate throughput capacity, they can not be used to estimate the actually achievable capacity performance which provides more meaningful insights for network designers.

This thesis studies the exact throughput capacity in 3D MANETs under the gen-

eral two-hop relay routing algorithm with packet redundancy [10, 51] techniques, which is first proposed in chapter 3. Under the routing algorithm, a source node first replicate packet waiting for dispatching, and then dispatches at most f copies of this packet to different relay nodes that help to forward them to the destination node.

2.4 Other Studies of 3D MANETs

In this section, we present other available works in 3D MANETs, which mainly focus on the studies of routing algorithms. The common limitation of these works is that they only provide the simulated results of the packet delivery performance, while the analytical performance study is largely neglected [54–60].

Durocher *et al.* in [54] modeled a three-dimensional ad hoc network by a unit ball graph, where nodes are located in three-dimensional space, and for each node has an edge between this node to every node in the unit-radius ball.v, there was an edge between v and every node u contained in the unit-radius ball centred at v. They showed that for any fixed k, there can be no k-local routing algorithm that guarantees delivery on all unit ball graphs. This result is in contrast with the two dimensional case, where 1-local routing algorithms that guarantee delivery are known.

Alshabtat *et al.* in [55] proposed a routing protocol named Directional Optimized Link State Routing Protocol (DOLSR) for Unmanned Aerial Vehicles (UAVs). This protocol is based on the well known protocol which been called Optimized Link State Routing Protocol (OLSR). A heuristic also developed that allowed DOLSR protocol to minimize the number of the multipoint relays. Simulation by OPNET network simulation tool showed that their protocol outperformed Optimized Link State Routing Protocol(OLSR), Dynamic Source Routing (DSR) protocol and Ad Hoc On demand Distance Vector (AODV) routing protocol in reducing the end-to-end delay and enhancing the overall throughput. In this paper, the authors provided the DOLSR routing protocol block diagram and simulation results rather than theoretical model.

He *et al.* in [56] proposed a novel routing protocol named Complex Three-dimensional scenario oriented Routing (C-TDR) for the complex 3D scenarios. This

protocol takes into account the 3D distribution of nodes and the characteristics of fluctuant transmission range of nodes in 3D VANET. Thus, it more fitting the realistic scenario and ensures the overall routing performance. Simulation results showed that C-TDR increased the packet delivery rate and decreased the end-to-end delay and hop count. In this paper, the authors provided pseudo-code of proposed protocol and simulation results rather than theoretical model.

THIS PAGE INTENTIONALLY LEFT BLANK

Chapter 3

Preliminaries

In this chapter, we first introduce system models of this thesis, including network model, mobility model and communication model, and then we introduce two-hop relay algorithm with packet redundancy. Finally, we introduce transmission-set based scheduling scheme adopted in this thesis.

3.1 System Models

3.1.1 Network and Mobility Models

We consider network with n mobile nodes uniformly distributed in a unit cube area. The cube area is evenly divided into $m \times m \times m$ equal-sized cells, as shown in Figure 3-1, Time is slotted into fixed-length slots [10, 22, 49, 61–63]. The nodes in the network move among these cells following the widely used independently and identically distributed (i.i.d.) mobility model [10, 22, 49, 61, 62, 64]. According to the i.i.d. mobility model, at the beginning of each time slot, every node independently selects one from all m^3 cells with the equal probability to move into, and stays at the selected cell for the rest of the time slot.

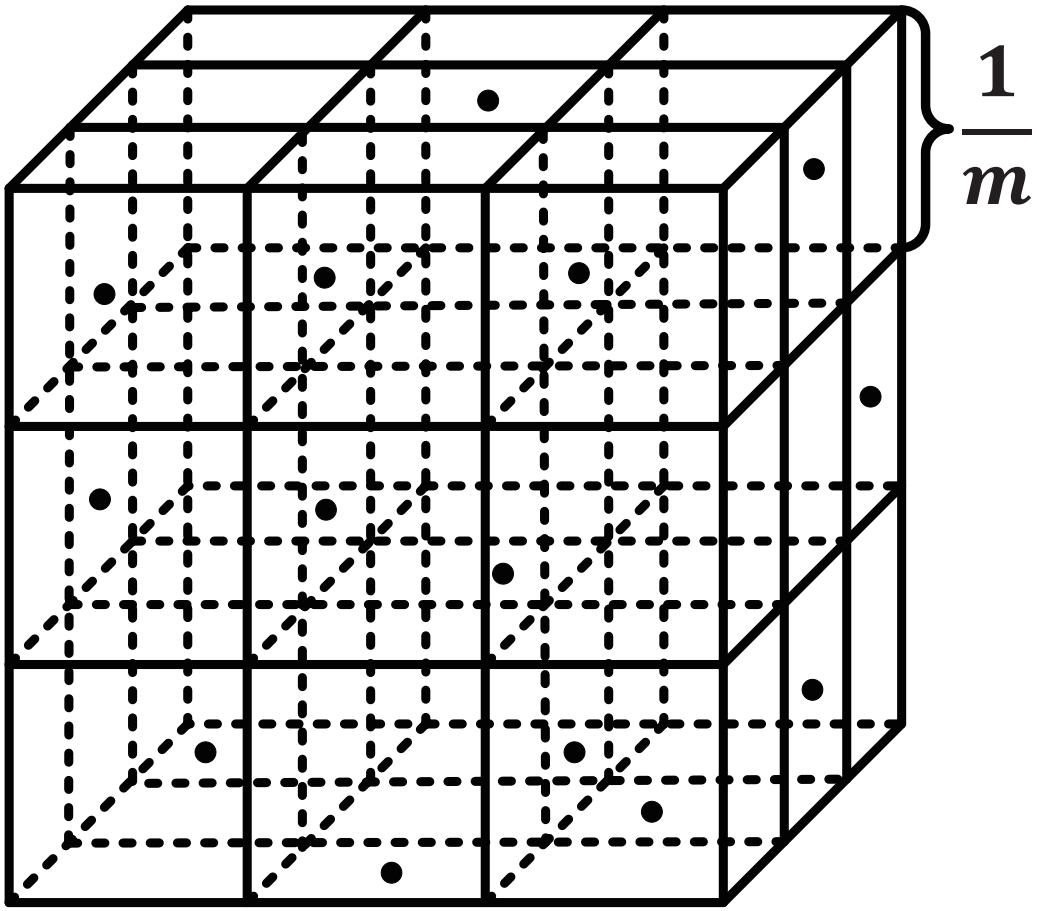

Figure 3-1: Network model

3.1.2 Communication Model

Similar to previous studies [20, 22, 50, 65], we consider a Local Transmission Scenario where a transmitting node (transmitter) can only transmit to those nodes (receivers) in the same cell or in its 26 adjacent cells. Two cells are called adjacent cells if they share a common vertex.

To avoid interferences from other transmitters in the same time slot, we adopt the widely used Protocol Model [66] here. Suppose that all the nodes employ the same fixed transmission range r, at some time slot t a node T_x is transmitting to another node R_x. We use $d_{T_x R_x}(t)$ to denote Euclidean distance between T_x and R_x. To guarantee the transmission from T_x to R_x to be successful at the time slot, the following two conditions should hold according to the Protocol Model:

1. $d_{T_x R_x}(t) \leq r$,

2. $d_{T_k R_x}(t) \geq (1+\Delta)r$ for every other node T_k transmitting simultaneously at the same time slot t,

where guard-factor Δ is a positive number for interference prevention. We assume that the total number of bits transmitted per time slot is fixed and normalized to one packet.

3.1.3 Traffic Model

Similar to [10, 23, 67–69], we adopt the permutation traffic pattern in our study. Under this traffic model, there are in total n distinct source-destination pairs in the considered MANET, i.e. $1 \rightarrow 2, 2 \rightarrow 3, ..., (n-1) \rightarrow n, n \rightarrow 1$. Here for $T_x = 1, ..., n-1$, node T_x generates traffic destined for node $T_x + 1$ and node n generates traffic destined for node 1. Therefore, each node is a source of its locally generated transmission flow and also a destination of a transmission flow originated from another node. Each node can serve as a potential relay that helps to forward packet for other $n-2$ transmission flows.

3.2 Two-hop Relay Algorithm with Packet Redundancy

Since Grossglauser and Tse for the first time adopted the two-hop relay scheme in [67], this scheme and its variants have become a class of attractive routing scheme for ad hoc mobile networks. This is because they are simple yet efficient, further more, they enable the capacity and delay to be studied analytically. As illustrated in Figure 3-2, packet transmission in the two-hop relay scheme is divided into two Phases, in Phase 1, the source node transmits a packet to an intermediate node (relay node), and then in Phase 2 the relay node transmits the packet to destination node. Since the source node can directly transmit a packet to its destination node once such transmission

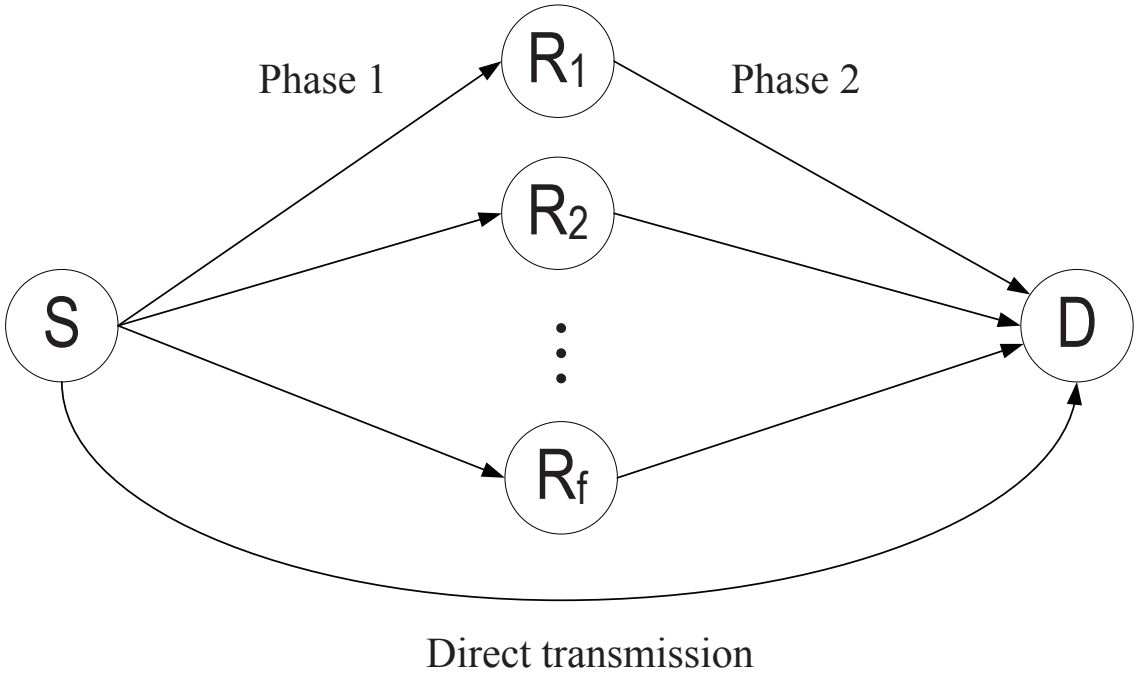

Figure 3-2: Illustration of two-hop relay with packet redundancy.

opportunity arises, every packet goes through at most two hops to reach its destination in a two-hop relay network.

3.2.1 Packet Redundancy Technique

Packet redundancy technique is an effective approach which can increase packet transmission opportunity. The main idea of packet redundancy is that a packet has multiple copies. This technique has been widely applied in MANETs routing algorithm research. Spyropoulos *et al.* explored the network performance adopting one-copy redundancy and multiple-copy redundancy technique in [70] and [71], respectively.

3.2.2 Two-hop Relay Algorithm with Packet Redundancy

We adopt two-hop relay algorithm with packet redundancy (2HR-f) for packet routing. Here we briefly describe the packet delivery processing to help understanding the algorithm. Without loss of generality, we focus on a tagged transmission flow, and denote its source node and destination node as S and D, respectively. The source

node S will individually deliver at most f copies of a packet to distinct relay nodes, the destination D may receive the packet from either source S or one relay node R. It is easy to see that in a 2HR-f network each packet will have at most $f + 1$ copies including the original one in its source node.

Each node may act as relay for other $n - 2$ transmission flows (here minus 2 corresponds to these two cases when the node is the source or destination for the transmission flow) in the 2HR-f network. Thus, to support the operation of the algorithm, each node is equipped with n individual queues at its buffer: one send-queue for storing the packets that are locally generated at the node and waiting for their copies to be distributed, one already-sent queue for storing packets whose f copies have already been distributed out but their reception statuses are not confirmed yet (from destination node), and $n-2$ parallel relay-queues for storing packets of other transmission flows (one queue per transmission flow). Furthermore, we assume that these n queues are first in first out queues, and each queue is assumed to have enough buffer space.

We adopt the mechanism which has been discussed previously to overcome the redundant packet problem. For the tagged transmission flow, each packet P at the send-queue in the source node S was labeled with a *send number* $SN(P)$. Similarly, the destination node D also maintains a *request number* $RN(D)$ which indicates the send number of the currently request packet, such that each packet is received in order at the node D and the packets which have been received are removed from already-sent queue.

The 2HR-f algorithm can be formally summarized as the following Algorithm 1.

Remark 1. *It is noted that the network topology of 3D MANETs is severely dynamic as nodes in the network can move freely to any direction of the 3D space. Due to this reason, we did not adopt the ACK (Acknowledgement) mechanism in this thesis to guarantee that the packet has reached its destination. Similar to [1, 10, 15, 49], we assume in this thesis that whenever the receiver is within the transmission range of the transmitter, the packet can be successfully received by the receiver. Thus, the destination node can receive the packet from either the source node or a relay node*

Algorithm 1 2HR-f Algorithm:

1. **if** the node S is selected as transmitter **then**
2. **if** the node D is within transmission range of S **then**
3. S executes Procedure 1 with D;
4. **else**
5. S randomly selects one node (say V) from these nodes in its transmission range.
6. P_r ={0,1};
7. **if** $P_r = 0$ **then**
8. S executes Procedure 2 with V;
9. **else**
10. S executes Procedure 3 with V;
11. **end if**
12. **end if**
13. **end if**

Procedure 1 $S \rightarrow D$ transmission:

1. S initiates a handshake to obtain the $RN(D)$ from node D;
2. **if** $SN(P) > RN(D)$ **then**
3. S retrieves the packet P with $SN(P) = RN(D)$ from its already-sent-queue
4. S sends the P to node D;
5. **else if** $SN(P) = RN(D)$ **then**
6. S sends P directly to node D;
7. **else**
8. S sends to node D the packet waiting right behind P in the send-queue;
9. **end if**
10. S deletes all packets with $SN \leq RN(D)$ inside the already-sent-queue and send-queue;
11. S update $SN(P)$, i.e., set $SN(P) = SN(P + 1)$;

Procedure 2 $S \rightarrow R$ transmission:

1. S initiates a handshake with node V;
2. **if** V has one copy of P **then**
3. S remains idle;
4. **else**
5. S sends a copy of packet P to V;
6. **if** f copies of packet P have been sent out to relay nodes **then**
7. S puts P to the end of its already-sent-queue;
8. S updates $SN(P)$, i.e., set $SN(P) = SN(P + 1)$;
9. **end if**
10. V puts P at the end of its relay-queue dedicated to node D;
11. **end if**

Procedure 3 $R \rightarrow D$ transmission:

1. S initiates a handshake to obtain the $RN(V)$ from node V;
2. **if** S has a packet P in the relay-queue dedicated to V with $SN(P) = RN(V)$ **then**
3. S sends packet P to node V;
4. **else**
5. S remains idle;
6. **end if**
7. S deletes all packets with $SN \leq RN(V)$ from its relay-queue dedicated to V;

in its transmission range, and the packet can always reach its destination after it is transmitted from the source node.

3.3 Transmission Scheduling Scheme

To support as many simultaneous transmissions as possible without interfering with each other in 3D MANETs, we adopt a transmission-set based scheduling scheme [65, 72]. Under this scheduling scheme with parameter α, a transmission-set is a subset of cells where any two cells have a distance of some multiples of α cells in three directions along the x, y and z axes, respectively, and all the cells there could transmit simultaneously without interfering with each other. According to the definition of transmission-set, all m^3 cells are actually divided into α^3 distinct transmission-sets. Figure 3-3 shows an example of $m = 12$ and $\alpha = 4$, where there are 64 transmission-sets in total and all shaded cells belong to the same transmission-set. We assume that each transmission-set can get transmission opportunity in turn in every α^3 time slots, thus each cell in the transmission-set gets transmission opportunity as well. We call a cell an active cell if it gets transmission opportunity. In a time slot, if more than one nodes are residing in an active cell, only one node is randomly selected as the transmitter (transmitting node).

To guarantee that these transmitting nodes in all the cells of a transmission-set can transmit simultaneously without interfering with each other, we need to properly determine the parameter α. According to the mentioned Local Transmission Scenario [67], where a node in an active cell can transmit to another node in the same

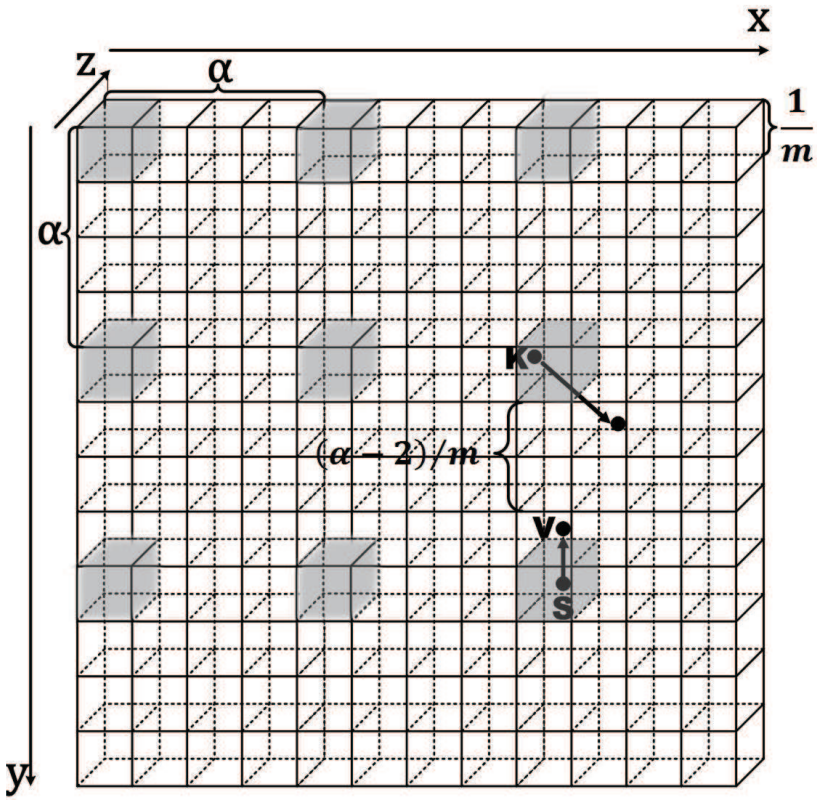

Figure 3-3: Illustration of a transmission-set with $m = 12$ and $\alpha = 4$, where all the shaded cells in the directions of x and y axes belong to the same transmission-set. In the same transmission-set, the shaded cells in the direction of z axis is not shown for simplicity.

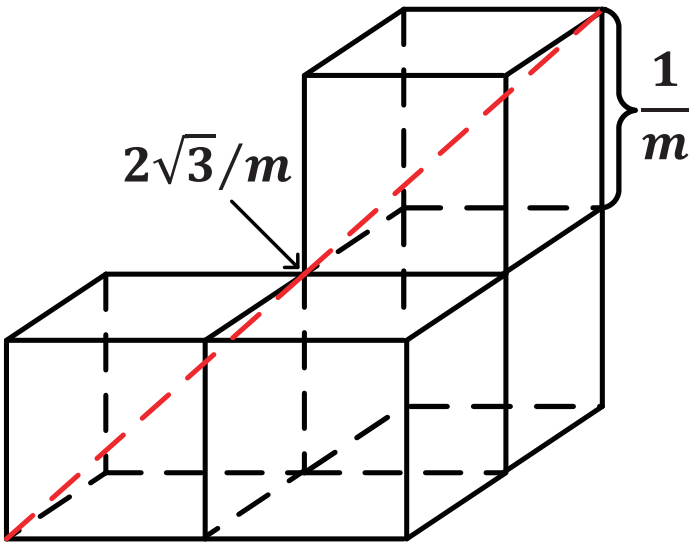

Figure 3-4: The maximum transmission distance between a transmitting node and its receiving node

cell or in its 26 adjacent cells. Thus, the maximum transmission distance (denoted as r) from a node to another node is calculated as $2\sqrt{3}/m$, as shown in Figure 3-4. Due to the wireless interference, only these nodes that are sufficiently far away could simultaneously transmit without interfering with each other. As shown in Figure 3-3, suppose that a node S in an active cell is transmitting to another node V, any other transmitting node K in the same transmission-set is at least $(\alpha - 2)/m$ away from V. According to the Protocol Model [66], we have

$$(\alpha - 2)/m \geq (1 + \Delta) \cdot r. \tag{3.1}$$

Substituting $r = 2\sqrt{3}/m$ into (3.1) yields

$$\alpha \geq (1 + \Delta)2\sqrt{3} + 2. \tag{3.2}$$

Since α is an integer and $\alpha \leq m$, we have

$$\alpha = \min\left\{\left\lceil(1 + \Delta)2\sqrt{3}\right\rceil + 2, m\right\} \tag{3.3}$$

where $\lceil x \rceil$ is ceiling function, returning the smallest integer no smaller than x.

3.4 Summary

In this chapter, we introduced the network model, the i.i.d. mobility model, the traffic model, two-hop relay algorithm with packet redundancy, transmission-set based scheduling scheme.

THIS PAGE INTENTIONALLY LEFT BLANK

Chapter 4

Packet Delivery Probability Study in 3D MANETs

The study of packet delivery probability performance in 3D MANETs is critical for supporting future various applications in such networks. This chapter explores the packet delivery probability in 3D MANETs under a two-hop relay algorithm with packet redundancy. This chapter first develops a Markov chain-based theoretical framework to model the packet delivery process under the algorithm and then determines some basic probabilities related to packet delivery process. With the help of the theoretical framework and related basic packet delivery probabilities, the analytical expression is further derived for packet delivery probability.

4.1 Performance Metric

For a given packet lifetime τ, the delivery probability is defined as the probability that the destination node receives the packet before the lifetime expires.

4.2 Markov Chain Theoretical Framework

In this section, we develop a Markov chain theoretical framework to depict the packet delivery process under two-hop relay algorithm with packet redundancy, and derive

some related basic transmission probability results.

4.2.1 Markov Chain Theoretical Framework

For a tagged transmission flow with source node S and destination node D and a given packet, we use i $(1 \leq i \leq f+1)$ to denote a general transient state under which there are in total i copies of the packet in the network (including one original packet in the source node). According to the operations of the routing algorithm proposed in chapter 3, for a transient state i at current time slot, only one of the following five transmission scenarios may happen in the next time slot:

- SD Scenario: Source-to-Destination transmission, i.e., S will successfully transmit the packet to D.
- SR Scenario: Source-to-Relay transmission only, i.e., S will successfully transmit the packet to a relay node while none of relay nodes transmits the packet to D.
- RD Scenario: Relay-to-Destination transmission only, i.e., A relay node will successfully transmit the packet to D while S fails to transmit the i-th copy to relay node.
- SR+RD Scenario: both simultaneous Source-to-Relay and Relay-to-Destination transmissions, i.e., these two transmissions will happen simultaneously.
- Selfloop Scenario: a state will transit to itself.

If we use A to denote an absorbing state indicating that D has received the packet at this state, then the packet delivery process under the algorithm can be modeled as a finite state absorbing Markov chain as shown in Figure 5-1.

In Figure 4-1, for the case of the state 1, it represents that there is only one packet in the network, i.e., the original packet in the source node, thus one of these three transitions of SD Scenario, SR Scenario and Selfloop Scenario may happen in the next time slot. From this state to absorbing state, only in SD Scenario.

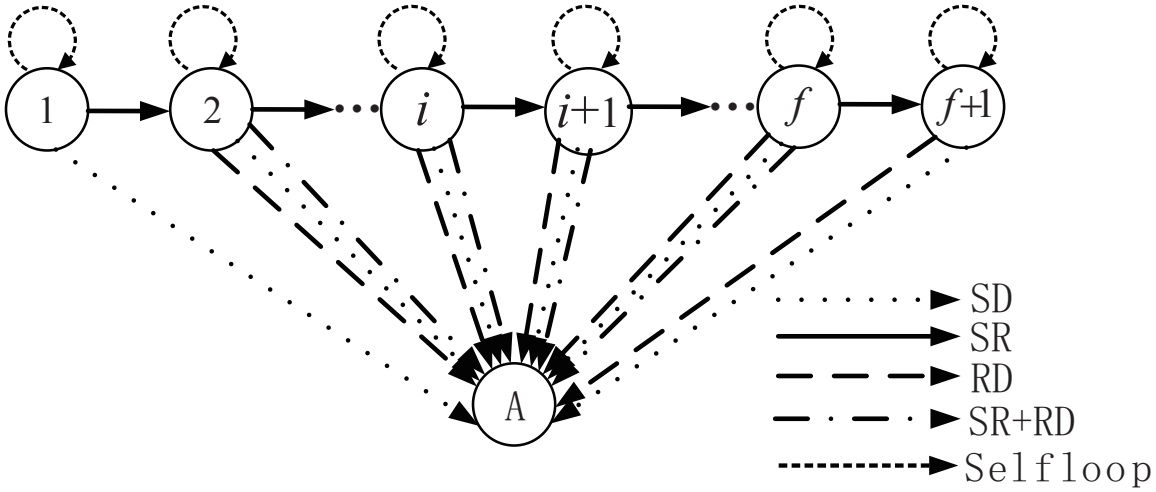

Figure 4-1: Absorbing Markov chain theoretical framework.

For the case of each state between states 2 and f, it represents that the source node has not transmitted out all f copies of the packet and some relay nodes are carrying the copies, thus one of these five transitions of SD Scenario, SR Scenario, RD Scenario, $SR+RD$ Scenario, and Selfloop Scenario may happen in the next time slot.

For the case of the state $f+1$, it represents that there are $f+1$ copies of the packet in the network, where the source node has already transmitted out all f copies to distinct relay nodes such that it will not perform Source-to-Relay transmission, thus one of these three transitions of SD Scenario, RD Scenario and Selfloop Scenario may happen in the next time slot.

As shown in Figure 4-1, it is notable that for the tagged transmission flow and a given packet, suppose that the current state i will transit to itself in the next time slot, it means that the corresponding transmitting node does not transmit the packet to another node. Here the current state i represents that there are in total i copies of the packet in the network (including the original one at the source node). For example, if the current state is 1, then the transmitting node (i.e.,the source node) does not transmit the packet to a relay node or its destination node in the next time slot.

4.2.2 Some Basic Transmission Probabilities

Lemma 1. *For a given time slot and a tagged transmission flow, the probability that the source node S conducts a Source-to-Destination transmission and the probability that the S conducts a Source-to-Relay or Relay-to-Destination transmission, denote by p_{sd}, p_{srd}, respectively. Then we have*

$$\begin{aligned} p_{sd}=&\frac{1}{\alpha^3}\Big\{\sum_{k=0}^{n-2}\binom{n-2}{k}\Big(\frac{1}{m^3}\Big)^k\Big(\frac{m^3-1}{m^3}\Big)^{n-2-k}\frac{1}{m^3}\frac{1}{k+2} \\ &+\sum_{k=0}^{n-2}\binom{n-2}{k}\Big(\frac{1}{m^3}\Big)^k\Big(\frac{m^3-1}{m^3}\Big)^{n-2-k}\frac{26}{m^3}\frac{26}{k+1}\Big\} \end{aligned} \tag{4.1}$$

$$\begin{aligned} p_{srd} =& \frac{m^3-27}{m^3\alpha^3}\Big\{\sum_{k=1}^{n-2}\binom{n-2}{k}\Big(\frac{1}{m^3}\Big)^k\Big(\frac{m^3-1}{m^3}\Big)^{n-2-k}\frac{1}{k+1} \\ &+\sum_{k=1}^{n-2}\binom{n-2}{k}\Big(\frac{26}{m^3}\Big)^k\Big(\frac{m^3-27}{m^3}\Big)^{n-2-k}\Big\} \end{aligned} \tag{4.2}$$

Lemma 2. *For a given time slot and a tagged transmission flow, suppose that source node S is sending the j-th copy of the packet (i.e., $j-1$ relay nodes have carried the copy of packet) that destination node D is requesting for, and the remaining lifetime of the packet is no less than one time slot. We use $P_d(j)$,$P_r(j)$ and $P_{sim}(j)$ to denote the probability that S will successfully send a copy of the packet to a relay node which no carrying the packet, the probability that D will receive the packet, and the probability that both Source-to-Relay and Relay-to-Destination transmissions happen simultaneously, respectively, in the next time slot. Then we have*

$$P_d(j) = \frac{n-j-1}{2(n-2)}\cdot p_{srd} \tag{4.3}$$

$$P_r(j) = p_{sd} + \frac{j-1}{2(n-2)}\cdot p_{srd} \tag{4.4}$$

$$P_{sim}(j) = \frac{(j-1)(n-j-1)(m^3-\alpha^3)}{4m^3\alpha^6} \sum_{k=0}^{n-5} \binom{n-5}{k} h(k) \cdot \left\{ \sum_{t=0}^{n-4-k} \binom{n-4-k}{t} h(t) \left(1 - \frac{54}{m^3}\right)^{n-4-k-t} \right\} \quad (4.5)$$

where

$$h(x) = \frac{27(\frac{27}{m^3})^{x+1} - 26(\frac{26}{m^3})^{x+1}}{(x+1)(x+2)} \quad (4.6)$$

The proofs of lemma 1 and lemma 2 can be found in the Appendix A.

4.3 Packet Delivery Probability Modeling

Before deriving the packet delivery probability, we first define the packet delivery delay.

Definition 1. *The delivery delay of a packet is defined as the time duration starting from the time slot when source node S starts to deliver the first copy of the packet to the time slot when destination D has received this packet.*

For the tagged transmission flow, if we denote by D_t the packet delivery delay and denote by ρ the message delivery probability under the message lifetime constraint τ, then we have

$$\rho = P_r(D_t \leq \tau) = \sum_{t=1}^{\tau} P_r(D_t = t) \quad (4.7)$$

Here $P_r(D_t = t)$ in (4.7) denotes the probability that the packet or a copy of this packet arrives at the destination D by the end of the t_{th} time slot, i.e., the probability that the Markov chain gets absorbed by the end of the t_{th} time slot. Given that the Markov chain starts from the first state, i.e., state 1, according to the Markov chain theory [73], then we have

$$P_r(D_t = t) = \sum_{i=1}^{f} q_{1i}^{(t-1)} \cdot r_{i1} \quad (4.8)$$

where $q_{ij}^{(t)}$ denotes the probability that by the end of the t_{th} time slot the Markov chain is in the j_{th} state given that the Markov chain starts from the i_{th} state. Combining with the fact that $q_{ij}^{(t)}$ is actually the ij-entry of the matrix $\mathbf{Q}^t$, i.e., $\mathbf{Q}^t = (q_{ij}^{(t)})_{f\times f}$, (13) can be further transformed as

$$P_r(D_t = t) = \mathbf{e} \cdot \mathbf{Q}^{t-1} \cdot r_{i1} \tag{4.9}$$

here $\mathbf{e} = (1, 0, ..., 0)$.

Substituting (4.9) into (4.7), then we have

$$\begin{aligned} \rho &= \sum_{t=1}^{\tau} \mathbf{e} \cdot \mathbf{Q}^{t-1} \cdot r_i = \mathbf{e} \cdot (\mathbf{I} - \mathbf{Q})^{-1} \cdot (\mathbf{I} - \mathbf{Q}^{\tau}) \cdot \mathbf{R} \\ &= \mathbf{e} \cdot \mathbf{N} \cdot (\mathbf{I} - \mathbf{Q}^{\tau}) \cdot \mathbf{R} \end{aligned} \tag{4.10}$$

The Markov chain in Figure 4-1 clearly indicate that there are $f + 1$ transient states and one absorbing state, in total $f + 2$ distinct states. We number these states sequentially with $1, 2, ...f + 1, f + 2$ sequence numbers, then sequence numbers $1, 2, ...f + 1$ correspond to transient state, sequence number $f + 2$ corresponds to absorbing state. According to the absorbing Markov chain theory [74], we arrange these states in a left-to-right and top-to-down way, and we can get the one-step transition matrix P of the absorbing Markov chain.

$$\mathbf{P} = \begin{bmatrix} \mathbf{Q} & \mathbf{R} \\ \mathbf{0} & \mathbf{1} \end{bmatrix} \tag{4.11}$$

From 4.10 we can see that in order to get the packet delivery probability ρ, we have to derive the $\mathbf{N}$ and $\mathbf{R}$. We derive the matrices $\mathbf{N}$ first, and the critical part of this issue is to derive the matric $\mathbf{Q}$ since $\mathbf{N} = (\mathbf{I} - \mathbf{Q})^{-1}$ and $\mathbf{I}$ is the identity matrix, thus

we arrange $\mathbf{Q}$ as the following partitioned matrices

$$\mathbf{Q} = \begin{bmatrix} \mathbf{Q}_0 & \mathbf{Q}'_0 & & & & & & \\ & \mathbf{Q}_1 & \mathbf{Q}'_1 & & & & & \\ & & \ddots & \ddots & & & & \\ & & & \mathbf{Q}_k & \mathbf{Q}'_k & & & \\ & & & & \ddots & \ddots & & \\ & & & & & \mathbf{Q}_f & \mathbf{Q}'_f & \\ & & & & & & \mathbf{Q}_{f+1} \end{bmatrix}, \tag{4.12}$$

Here $\mathbf{Q}$ is an $(f+1)$-by-$(f+1)$ matrix, its entry $q_{ij}(i, j \in [1, f+1])$ represents the one-step transition probabilities among $f+1$ transient states. The non-zero entry of matrix $\mathbf{Q}$, i.e., the one-step transition probabilities among transient states can be determined as

$$q_{ii} = \begin{cases} 1 - p_{sd} - \frac{p_{srd}}{2} + p_{sim}(i), & \text{if} \quad 1 \leq i \leq f, \\ 1 - P_r(f+1), & \text{if} \quad i = f+1. \end{cases} \tag{4.13}$$

$$q_{i,i+1} = P_d(i) - P_{sim}(i), \qquad 1 \leq i \leq f \tag{4.14}$$

$\mathbf{R}$ is a nonzero $(f+1)$-by-1 matrix, its entry $r_{ij}(i \in [1, f+1], j \in 1)$ represents the one-step transition probabilities from $f+1$ transient states to the absorbing state. The non-zero entry of matrix $\mathbf{R}$, i.e., the one-step transition probabilities from transient states to the absorbing state, can be determined as

$$q_{r,1} = P_r(i), \qquad 1 \leq i \leq f+1. \tag{4.15}$$

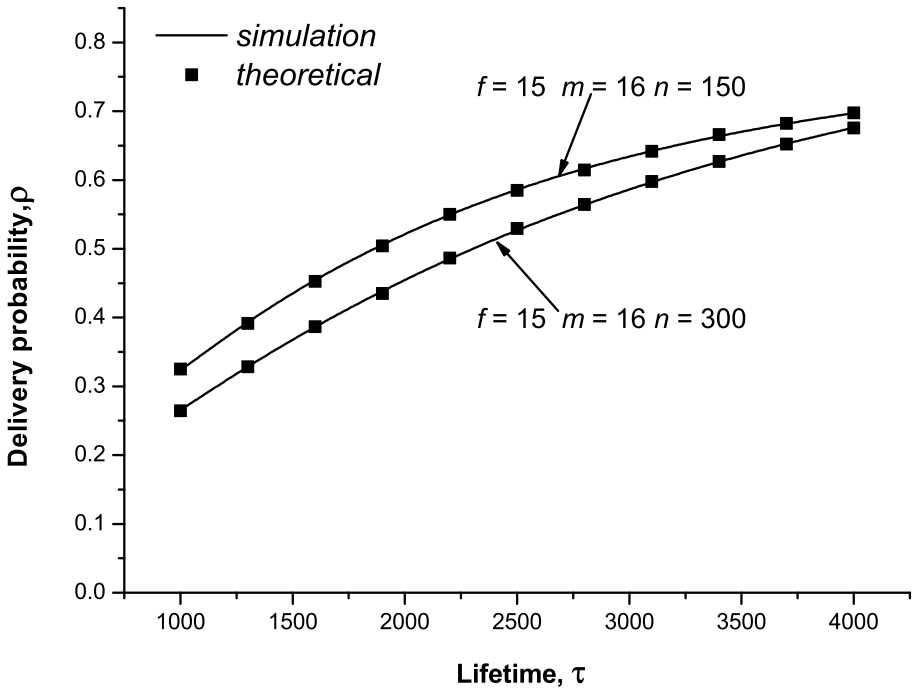

Figure 4-2: Theoretical packet delivery probability and simulation ones.

4.4 Number Results

4.4.1 Simulation Settings

In order to simulate the packet delivery process in a two-hop relay 3D MANET with packet lifetime, we developed a specific network simulator by C++. Similar to the settings adopted in [75], the guard factor Δ is set to 1, and hence the transmission-set is defined with $\alpha = \min\{9, m\}$.

4.4.2 Model Validation

Extensive simulation has been conducted to validate the theoretical delivery probability. Here we present the results of two network scenarios $\{m = 15, f = 16, n = 150\}$ and $\{m = 15, f = 16, n = 300\}$. As shown in Figure 4-2, the theoretical results

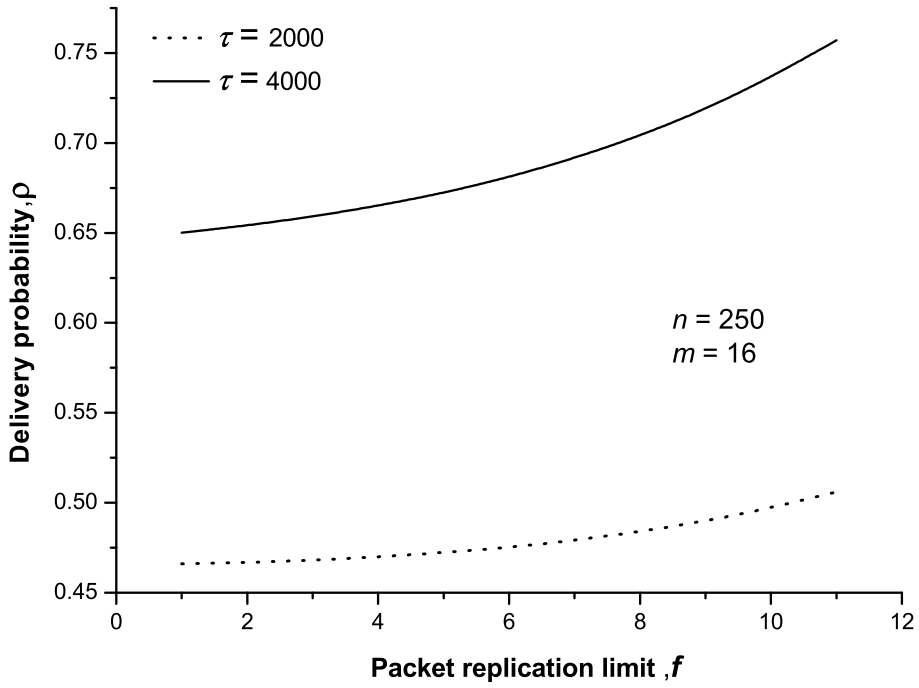

Figure 4-3: Illustration of the relationship between ρ and f.

match nicely with the simulation ones under two network scenarios . Therefore, our theoretical model can accurately predict the delivery probability performance under the two-hop relay scheme in the considered 3D MANETs.

4.4.3 Performance Analysis

We first explore how the delivery probability varies with packet redundancy limit f. We can see from Figure 4-3 that the delivery probability monotonically increases with f. Another observation from Figure 4-3 is that the variation tendencies of delivery probability are similar under both the two settings of $\tau = 2000$ and $\tau = 4000$. We proceed to explore how the delivery probability varies with number of nodes n. We can see from Figure 4-4 that the delivery probability first increases, and then decreases. This can be explained as follows: when n relatively small (e.g. $n < 40$), the network is sparse and the increasing of n could lead to the increasing of the transmission prob-

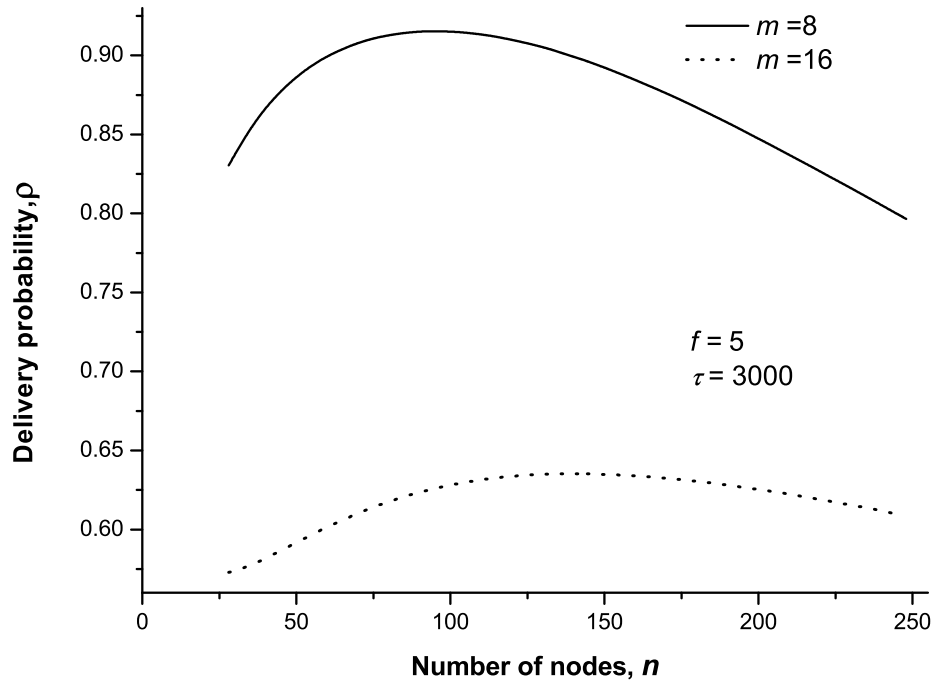

Figure 4-4: Illustration of the relationship between ρ and n.

ability. As n further increases d(e.g. $n > 90$), the network nodes become relatively densely distributed, interference and medium contention issues begin to dominate the delivery performance, and thus decrease the delivery probability. A further careful observation of Figure 4-4 indicates that for the same setting of f, a bigger parameter m could result in a lower delivery probability. It can be explained as follows: we know that the considered network area is divided into $m \times m \times m$ cells and the mobile nodes roam from one cell to another, which results in the nodes sparsely distributed in the network as m increases, and thus decreases the delivery probability.

We also attempt to study the packet delivery probability over the broadcast channel mode. When a node gets a transmission opportunity, it broadcasts the copies of the packet to the nodes which locate in the same cell or its 26 adjacent cells. The number of the broadcast is set to f for each packet. The simulation results are summarized in Figure 4-5. We can see from Figure 4-5 that the delivery probability of

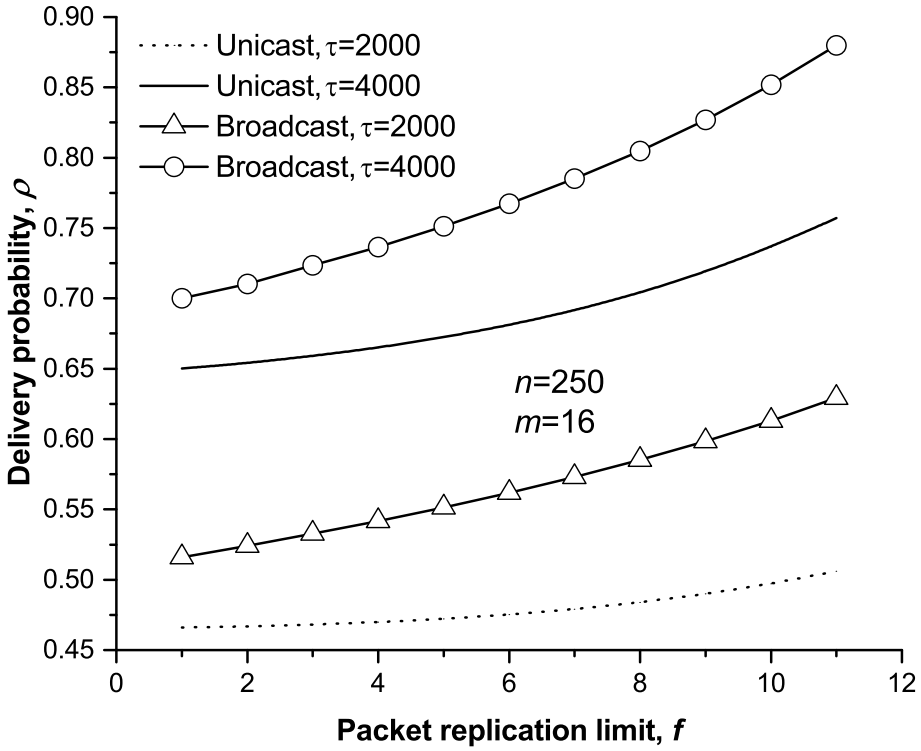

Figure 4-5: Packet delivery probability comparison between unicast and broadcast.

using broadcast is higher than using unicast.

Although the simulation results show that the delivery probability performance under broadcast is better than that under unicast. This thesis does not adopt the broadcast traffic pattern. This is because under such a traffic pattern, the number of relay nodes carrying the packet is unknown, which makes it more difficult to develop a Markov chain to analytically study the packet delivery performance.

4.5 Summary

In this chapter, we first develop a Markov chain theoretical framework to depict the packet delivery process under two-hop relay scheme with packet redundancy. With the help of the Markov chain theoretical framework, we then derive an analytical

expression for delivery probability under any given packet lifetime. Simulation results indicate that our theoretical model can accurately predict delivery probability performance in 3D MANETs.

Chapter 5

Packet Delivery Delay Study in 3D MANETs

Packet delivery delay in 3D MANETs is critical to support various applications in such networks. To study the packet delivery delay in 3D MANTEs, with the help of the Markov chain theoretical framework developed, analytical expressions are further derived for the mean and variance of packet delivery delay.

5.1 Markov Chain Theoretical Framework

In this section, we give some basic transmission probabilities. Their derivation processes are similar to these of the probabilities in Chapter 4, thus they are omitted here. We present some contents similar to what in Chapter 4 here to help understanding. And then we develop a Markov chain theoretical framework to depict the packet delivery process under 2HR-f algorithm.

5.1.1 Some Basic Transmission Probabilities

For an analytical study of packet delivery delay performance, we need to derive some basic transmission probabilities. Here we give the following two lemmas.

Lemma 3. *Consider a given time slot and a tagged transmission flow, the probability*

of source node S conducts a Source-to-Destination transmission and the probability that S conducts a Source-to-Relay or Relay-to-Destination transmission, denoted by p_{sd} and p_{srd}, respectively. Then we have

$$p_{sd}=\frac{1}{\alpha^3}\Big\{\frac{27-m^3}{n-1}+\frac{m^3}{n}-\frac{26}{n-1}\Big(\frac{m^3-1}{m^3}\Big)^{n-1} +\Big(\frac{m^3}{n-1}-\frac{m^3}{n}\Big)\Big(\frac{m^3-1}{m^3}\Big)^{n}\Big\} \tag{5.1}$$

$$p_{srd}=\frac{m^3-27}{m^3\alpha^3}\Big\{\sum_{k=1}^{n-2}\binom{n-2}{k}\Big(\frac{1}{m^3}\Big)^k\Big(\frac{m^3-1}{m^3}\Big)^{n-2-k}\frac{1}{k+1} +\sum_{k=1}^{n-2}\binom{n-2}{k}\Big(\frac{26}{m^3}\Big)^k\Big(\frac{m^3-27}{m^3}\Big)^{n-2-k}\Big\} \tag{5.2}$$

Lemma 4. *Consider a given time slot and a tagged transmission flow, at the current time slot, there have been g copies of the packet in network. In the next time slot, the probability that D will receive the packet, denoted by $P_r(g)$. The probability that D will successfully transmit a copy of the packet to a relay node which no carrying the packet, denoted by $P_d(g)$. The probability that both Source-to-Relay and Relay-to-Destination transmissions happen simultaneously, denoted by $P_{sim}(g)$. Then we have*

$$P_r(g)=p_{sd}+\frac{g-1}{2(n-2)}\cdot p_{srd} \tag{5.3}$$

$$P_d(g)=\frac{n-g-1}{2(n-2)}\cdot p_{srd} \tag{5.4}$$

$$P_{sim}(g)=\frac{(g-1)(n-g-1)(m^3-\alpha^3)}{4m^3\alpha^6}\sum_{k=0}^{n-5}\binom{n-5}{k}h(k) \cdot\Big\{\sum_{t=0}^{n-4-k}\binom{n-4-k}{t}h(t)\Big(1-\frac{54}{m^3}\Big)^{n-4-k-t}\Big\} \tag{5.5}$$

where

$$h(x) = \frac{27(\frac{27}{m^3})^{x+1} - 26(\frac{26}{m^3})^{x+1}}{(x+1)(x+2)} \tag{5.6}$$

5.1.2 Markov Chain Theoretical Framework

For a tagged transmission flow with source node S and destination node D and a given packet, we use i $(1 \leq i \leq f+1)$ to denote a general transient state under which there are in total i copies of the packet in the network (including one original packet at the source node). According to the operations of the algorithm, for a transient state i at current time slot, only one of the following five transmission scenarios may happen in the next time slot:

- SD Scenario: Source-to-Destination transmission, i.e., S will successfully transmit the packet to D.
- SR Scenario: Source-to-Relay transmission only, i.e., S will successfully transmit the packet to a relay node while none of relay nodes transmits the packet to D.
- RD Scenario: Relay-to-Destination transmission only, i.e., A relay node will successfully transmit the packet to D while S fails to transmit the i-th copy to relay node.
- SR+RD Scenario: both simultaneous Source-to-Relay and Relay-to-Destination transmissions, i.e., these two transmissions will happen simultaneously.
- Selfloop Scenario: a state will transit to itself.

If we use A to denote an absorbing state indicating that D has received the packet at this state, then the packet delivery process under the algorithm can be modeled as a finite state absorbing Markov chain as shown in Figure 5-1.

Remark 2. *As shown in Figure 5-1, for the tagged transmission flow and a given packet, suppose that the current state i will transit to itself in the next time slot,*

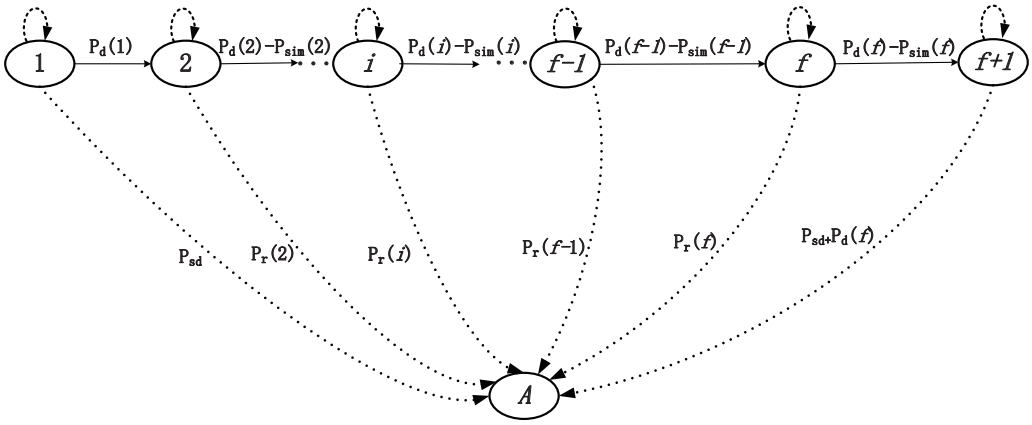

Figure 5-1: Absorbing Markov chain theoretical framework.

it means that the corresponding transmitting node does not transmit the packet to another node. Here the current state i represents that there are in total i copies of the packet in the network (including the original one at the source node). For example, if the current state is 1, then the transmitting node (i.e.,the source node) does not transmit the packet to a relay node or its destination node in the next time slot.

In Figure 5-1, for the case of the state 1, it represents that there is only one packet in the network, i.e., the original packet at the source node, thus one of these three transitions of SD Scenario, SR Scenario and Selfloop Scenario may happen in the next time slot.

For the case of the state $f+1$, it represents that there are $f+1$ copies of the packet in the network, where the source node has already transmitted out all f copies to distinct relay nodes such that it will not perform Source-to-Relay transmission, thus one of these three transitions of SD Scenario, RD Scenario and Selfloop Scenario may happen in the next time slot.

For the case of each state between states 2 and f, it represents that the source node has not transmitted out all f copies of the packet and some relay nodes are carrying the copies, thus one of these five transitions of SD Scenario, SR Scenario, RD Scenario, $SR+RD$ Scenario, and Selfloop Scenario may happen in the next time slot.

5.2 Packet Delivery Delay Modeling

With the help of the Markov chain theoretical framework and related basic transmission probability results in 5.1, this section gives the derivation process of the analytical expressions for expected value and relative standard deviation of packet delivery delay under the two-hop relay algorithm with packet redundancy. We first introduce the following definition of packet delivery delay.

Definition 2. *For a tagged transmission flow and a given packet, the delivery delay of a packet in considered 3D MANET is defined as time duration between the time slot that source node S starts to transmit the packet and the time slot that destination node D receives the packet.*

5.2.1 Expected Packet Delivery Delay

We use a_i to denote the time that the Markov chain takes to reach absorbing state A starting from the state i, where $1 \leq i \leq f+1$. We use q_{ij} to denote the probability that the state i transits to the state j, and then according to the theory of Markov chain [74], the expected value $E\{a_i\}$ of a_i is given by

$$E\{a_i\} = \frac{1 + \sum_{j \in [1, f+1], j \neq i} q_{ij} \cdot E\{a_j\}}{1 - q_{ii}}. \tag{5.7}$$

Thus, the expected value $E\{a_1\}$ of a_1 that just corresponds to the expected packet

delivery delay, can be determined as

$$E\{a_1\} = \frac{1 + \sum_{j\in[1,f+1],j\neq 1} q_{1j} \cdot E\{a_j\}}{1 - q_{11}} \tag{5.8}$$

$$= \frac{1 + P_d(1) \cdot E\{a_2\}}{P_d(1) + P_r(1)} \tag{5.9}$$

$$= \frac{1}{P_d(1) + P_r(1)} + \frac{P_d(1)}{P_d(1) + P_r(1)} \Big\{ \frac{1}{P_d(2) + P_r(2)} + \frac{P_d(2)}{P_d(2) + P_r(2)} E\{a_3\} \Big\} \tag{5.10}$$

$$= \frac{1}{P_d(1) + P_r(1)} + \frac{P_d(1)}{P_d(1) + P_r(1)} \frac{1}{P_d(2) + P_r(2)} + \frac{P_d(1)}{P_d(1) + P_r(1)} \frac{P_d(2)}{P_d(2) + P_r(2)} E\{a_3\} \tag{5.11}$$

We can see from Figure 5-1 that if $j > 2$, $q_{1j} = 0$, and if $j = 2$, $q_{1j} = P_d(1)$ because both q_{1j} and $P_d(1)$ denote the probability that SR Scenario happens, i.e., the source node can successfully transmit a copy of the packet to a relay node. We have

$$\sum_{j\in[1,f+1],j\neq 1} q_{1j} \cdot E\{a_j\} = P_d(1) \cdot E\{a_2\}. \tag{5.12}$$

Under the state 1, the Relay-to-Destination transmission will not happen in the next time slot, thus $P_r(1)$ denotes the probability that SD Scenario happens, i.e., the source node can successfully transmit the packet to its destination node. Since the q_{11} denotes the probability that the state 1 transits to itself, we have

$$1 - q_{11} = P_d(1) + P_r(1). \tag{5.13}$$

Substituting (5.12) and (5.13) into (5.8), then (5.9) follows.

Based on (5.7), we continue to iterate the formula(5.11), and then $E\{a_1\}$ is deter-

mined as

$$E\{a_1\}=\frac{1}{P_d(1)+P_r(1)}+\sum_{j=1}^{f-1}\Big\{\Big(\Pi_{k=1}^{j}\frac{P_d(k)}{P_d(k)+P_r(k)}\Big)\cdot\frac{1}{P_d(j+1)+P_r(j+1)}\Big\}+\Big(\Pi_{k=1}^{f}\frac{P_d(k)}{P_d(k)+P_r(k)}\Big)\cdot E\{a_{f+1}\} \tag{5.14}$$

where

$$E\{a_{f+1}\}=\frac{1}{P_r(f+1)} \tag{5.15}$$

5.2.2 Relative Standard Deviation

We use RSD and $\mathrm{Var}\{a_1\}$ to denote the relative standard deviation and variance of packet delivery delay, respectively. The RSD is defined as

$$RSD=\frac{\sqrt{Var\{a_1\}}}{E\{a_1\}}. \tag{5.16}$$

Since $\mathrm{Var}\{a_1\}$ can be determined as $\mathrm{Var}\{a_1\}=E\{{a_1}^2\}-\big(E\{a_1\}\big)^2$, and $E\{a_1\}$ can be determined by (5.14), we only need to derive the $E\{{a_1}^2\}$ here.

According to the definition of a_i, we can see that $E\{{a_i}^2\}$ is given by

$$\begin{aligned}E\{{a_i}^2\}&=\sum_{j=1}^{f+1}q_{ij}E\big\{(1+a_j)^2\big\}\\&=1+2\sum_{j=1}^{f+1}q_{ij}E\{a_j\}+\sum_{j=1}^{f+1}q_{ij}\cdot E\{{a_j}^2\}\end{aligned} \tag{5.17}$$

Let $\mathbf{a}^{(j)}=(E\{{a_1}^j,\},E\{{a_2}^j,\},\dots E\{{a_{f+1}}^j,\})^T$, then we can rearrange (5.17) as

$$\mathbf{I}\cdot\mathbf{a}^{(2)}=\mathbf{c}+2\mathbf{Q}\cdot\mathbf{a}^{(1)}+\mathbf{Q}\cdot\mathbf{a}^{(2)} \tag{5.18}$$

where $\mathbf{c}$ is the $(f+1)\times 1$ column vector with all entries being 1, i.e., $\mathbf{c}=\{1,1,\dots,1\}^T$.

Then, according to [74], we have

$$\mathbf{a}^{(1)} = (\mathbf{I} - \mathbf{Q})^{-1} \cdot \mathbf{c} \tag{5.19}$$

$$\mathbf{a}^{(2)} = (\mathbf{I} - \mathbf{Q})^{-1} \left\{ \mathbf{I} + \mathbf{2Q} \cdot (\mathbf{I} - \mathbf{Q})^{-1} \right\} \mathbf{c} \tag{5.20}$$

Since $E\{\mathbf{a_1}^2\} = \mathbf{e} \cdot \mathbf{a}^{(2)}$, where $\mathbf{e} = \{1, 0, \ldots, 0\}$, the $E\{a_1^2\}$ can be derived based on $\mathbf{Q}$.

Since the transitions in the Markov chain of Figure 5-1 happen only among the transient states of the same row or neighboring rows, the matrix $\mathbf{Q}$ there can be defined as

$$\mathbf{Q} = \begin{bmatrix} q_{1,1} & q_{1,2} & & & & & & \\ & q_{2,2} & q_{2,3} & & & & & \\ & & \ddots & \ddots & & & & \\ & & & q_{i,i} & q_{i,i+1} & & & \\ & & & & \ddots & \ddots & & \\ & & & & & q_{f,f} & q_{f,f+1} & \\ & & & & & & q_{f+1,f+1} \end{bmatrix}$$

The size of matrix $\mathbf{Q}$ is $(f+1) \times (f+1)$, the nonzero entries of matrix $\mathbf{Q}$ can be determined as

$$q_{i,i} = \begin{cases} 1 - p_{sd} - \frac{p_{srd}}{2} + P_{sim}(i), & \text{if} \quad 1 \leq i \leq f, \\ 1 - P_r(f+1), & \text{if} \quad i = f+1. \end{cases} \tag{5.21}$$

$$q_{i,i+1} = P_d(i) - P_{sim}(i), \quad \text{if} \quad 1 \leq i \leq f. \tag{5.22}$$

5.3 Numerical Results

In this section, we first provide simulation results to validate our theoretical models, and then illustrate the impact of network parameters on the packet delivery delay performance.

5.3.1 Simulation Settings

We developed a simulator using C++ language to simulate the packet delivery process under the two-hop relay algorithm with packet redundancy in 3D MANETs (now publicly available at [76]). The guard factor Δ in Protocol Model is fixed as $\Delta = 1$, and thus the transmission-set is defined with $\alpha = \min\{9, m\}$. Besides the simulation under i.i.d. mobility model considered in this chapter, we also implemented the simulator for the popular random walk model and random waypoint model, which are defined as follows.

- Random Walk Model [68]: At the beginning of each time slot, each node either stays inside its current cell or moves to one of its 26 adjacent cells, with the same probability 1/27.

- Random Waypoint Model [77]: At the beginning of each time slot, each node independently and randomly generates a three-dimensional vector $d = [d_x, d_y, d_z]$, where the values of d_x, d_y and d_z are uniformly drawn from $[1/m, 3/m]$. The node then moves a distance of d_x, d_y and d_z along the x-axis, y-axis and z-axis, respectively.

We focus on a tagged transmission flow with source node S and destination node D, and a given packet. The basic idea of the simulation for the packet delivery delay performance using C++ is included in the considered Algorithm 1. In Algorithm 1, we use Sim to denote the number of independent simulations, use $Total\_time$ to denote the sum of packet delivery delay in all Sim simulations, use $Time\_slot$ to denote the packet delivery delay in each simulation, use $delivery\_delay[t]$ to denote the packet delivery delay in the t_{th} simulation, and use $flag$ to denote whether or not D receives the given packet, where if D receives the given packet, and then $flag = 1$; otherwise, $flag = 0$.

Procedure 4 Simulated packet delivery delay performance:

1. **Input:** n nodes are randomly generated in the considered network; The number of independent simulations,$Sim = 10^6$;
2. **Output:** The packet delivery delay performance, $(E\{a_1\}, RSD)$;
3. $Total\_time = 0$;
4. **for** $t = 1$; $t <= Sim$; $t++$ **do**
5. $\quad Time\_slot = 0$, $flag = 0$;
6. $\quad$ **while** $(flag\ != 1)$ **do**
7. $\quad\quad Time\_slot++$;
8. $\quad\quad$ Each node updates its position according to node mobility model;
9. $\quad\quad$ Under the transmission-set based scheduling scheme, each node may be scheduled to perform a data transmission, where if D receives the given packet, and then $flag = 1$;
10. $\quad$ **end while**
11. $\quad delivery\_delay[t] = Time\_slot$;
12. $\quad Total\_time\ += Time\_slot$;
13. **end for**
14. The simulated standard deviation $Var\{a_1\}$ is the sample standard deviation, thus $Var\{a_1\} = \sqrt{\frac{1}{Sim-1}\sum_{t=1}^{Sim}(delivery\_delay[t] - E\{a_1\})}$;
15. $E\{a_1\} = Total\_time/Sim$;
16. $RSD = \frac{\sqrt{Var\{a_1\}}}{E\{a_1\}}$;

Remark 3. *Similar to previous studies [10, 78, 79], we consider that all the nodes in the network share a common half-duplex channel for data transmission and the total number of bits transmitted per time slot is fixed and normalized to one packet. It is notable that the network structure to switch from 2D to 3D becomes more complex. This is because in 3D MANET it involves not only highly dynamic topology, but also issues related to medium contention, node connectivity, data transmission, which leads to more complex theoretical analysis on the packet delivery delay performance.*

5.3.2 Model Validation

Extensive simulations were conducted to validate our theoretical models. Given the network scenario $\{m = 16, n = 60\}$ and when packet redundancy limit f varies from 1 to 10, the theoretical and simulated results are summarized in Figure 5-2. Figure 5-2 indicates that the simulation results under i.i.d. mobility model match nicely with the theoretical ones. Therefore, our theoretical model can accurately predict the packet delivery delay performance under the two-hop relay algorithm in 3D MANETs.

Another interesting observation from Figure 5-2 is that for the network scenario, the simulated packet delivery delay performance under the random walk and random waypoint models almost agree with those under the i.i.d. mobility model. According to the definitions of i.i.d., random walk and random waypoint mobility models, these three mobility models are different with each other. However, as shown in [10, 80], for a cell-partitioned network, the average delay under the i.i.d. mobility model is also identical to that under other non-i.i.d. mobility models only if they have the same steady-state distribution of nodes locations, like the random walk mobility model and random waypoint mobility model. Therefore, our theoretical models, although were developed for the packet delivery delay performance analysis under the i.i.d. mobility model, can also be used to predict the packet delivery delay performance in 3D MANETs under the random walk mobility model and random waypoint mobility model.

5.3.3 Performance Analysis

We first explore how the packet delivery delay performance $(E\{a_1\}, RSD)$ varies with the number of nodes n. As shown in Figure 5-3, for each setting of f, as n increases, the expected packet delivery delay first decreases, and then increases. This can be explained as follows: when n is relatively small, the network is sparse and the increasing of n could lead to the increasing of the probability that a packet is transmitted out and thus decreases the packet delivery delay. As n further increases, the network nodes become relatively densely distributed and the negative effects of interference

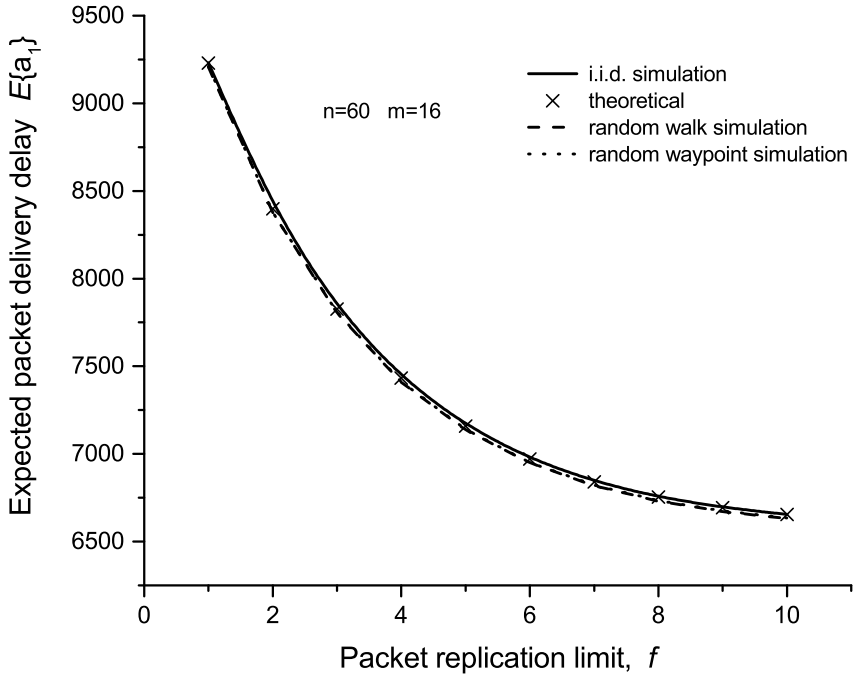

(a) $E\{a_1\}$ versus f in 3D MANET

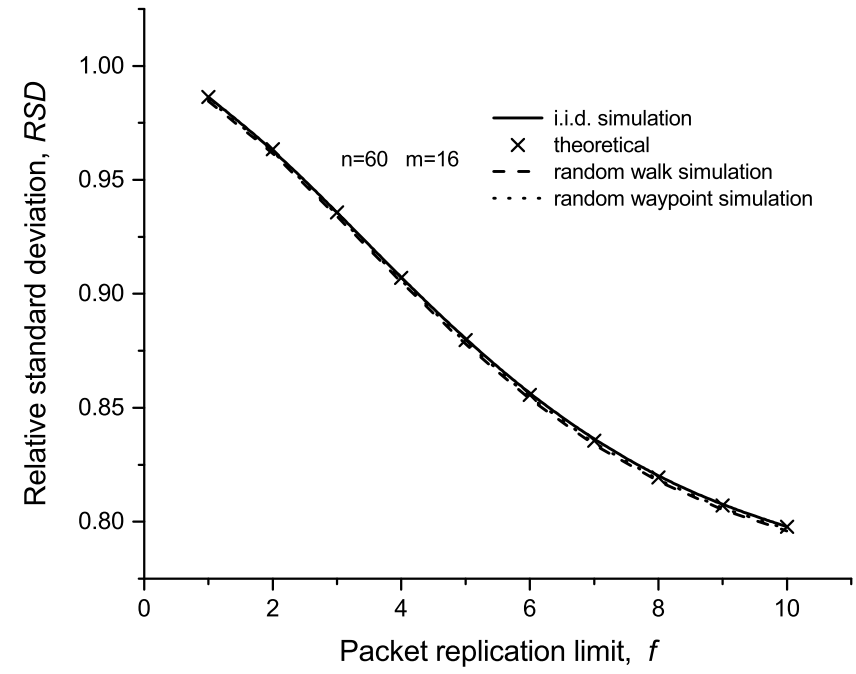

(b) RSD versus f in 3D MANET

Figure 5-2: Comparison between simulation results and theoretical ones for model validation.

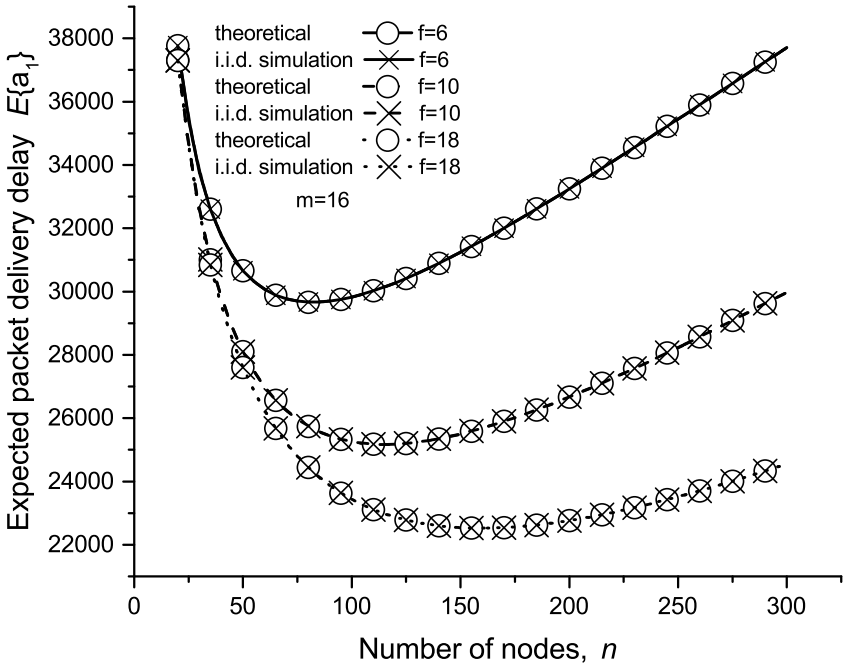

(a) $E\{a_1\}$ versus n in 3D MANET

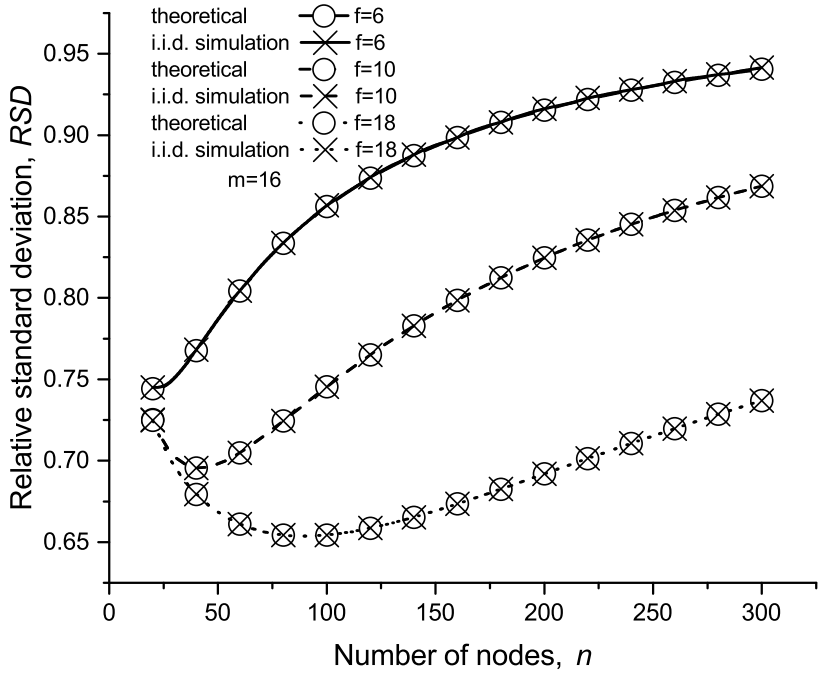

(b) RSD versus n in 3D MANET

Figure 5-3: The impact of number of nodes n on packet delivery delay performance in 3D MAENT

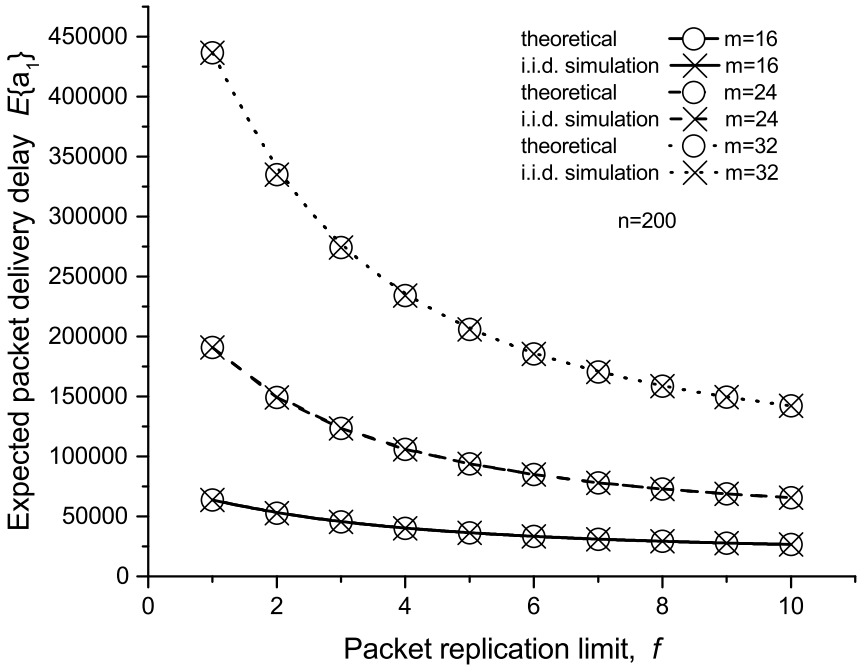

(a) $E\{a_1\}$ versus f in 3D MANET

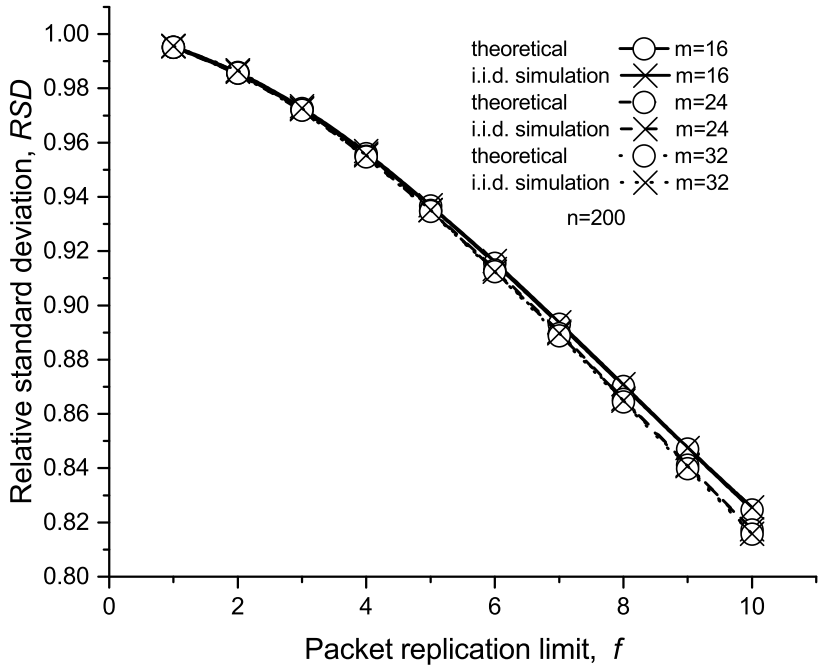

(b) RSD versus f in 3D MANET

Figure 5-4: The impact of packet redundancy limit f on packet delivery delay performance in 3D MANET

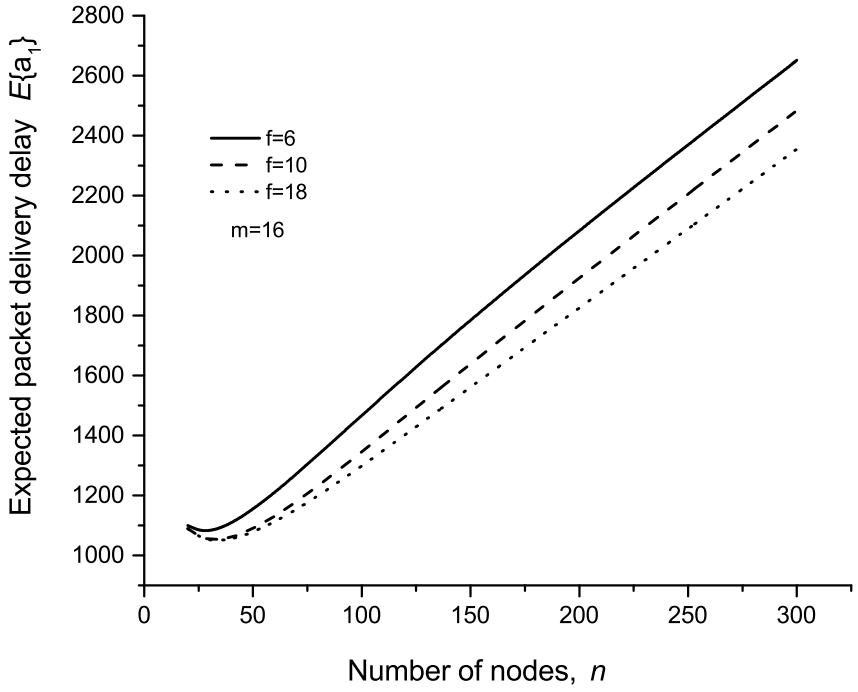

(a) $E\{a_1\}$ versus n in 2D MANET

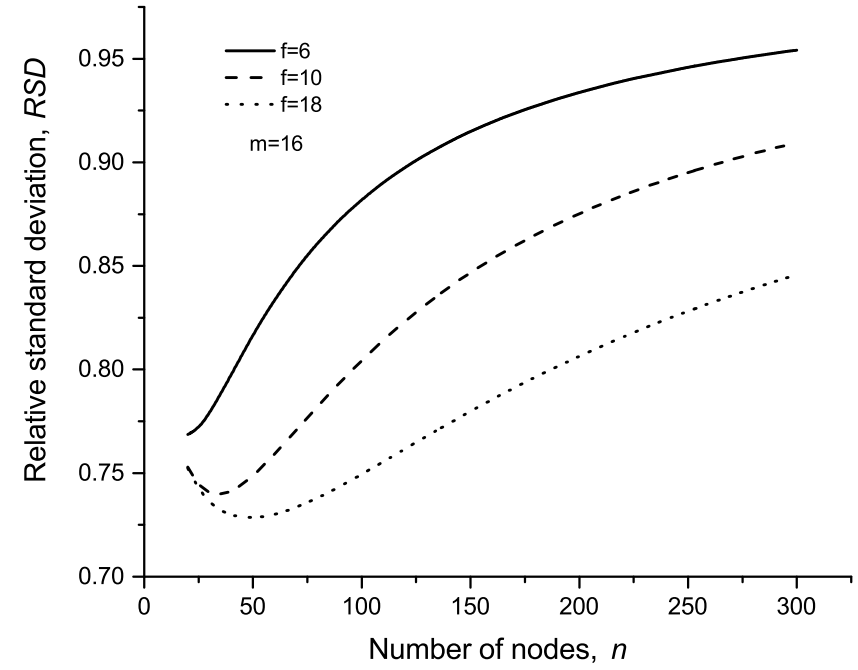

(b) RSD versus n in 2D MANET

Figure 5-5: The impact of number of nodes n on packet delivery delay performance in 2D MANET

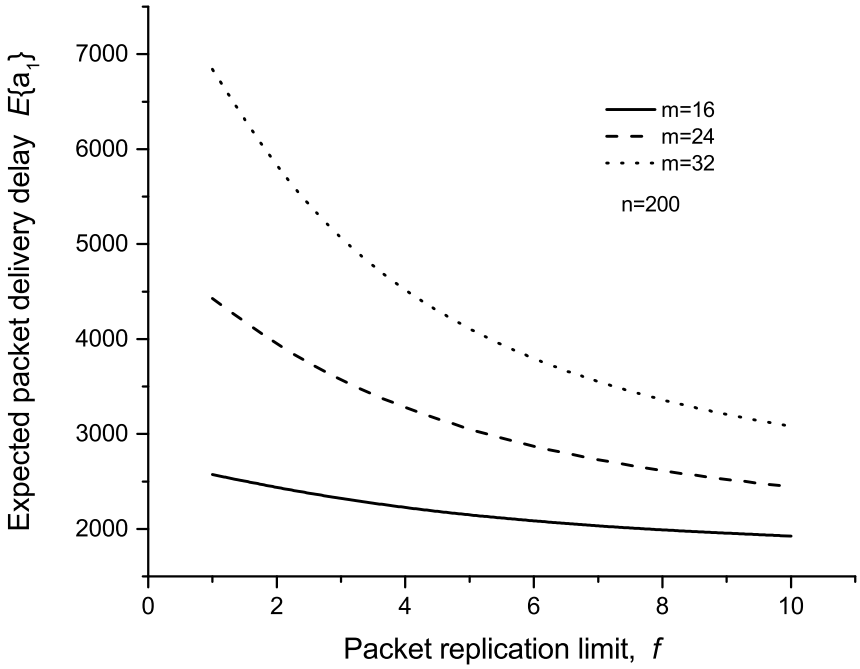

(a) $E\{a_1\}$ versus f in 2D MANET

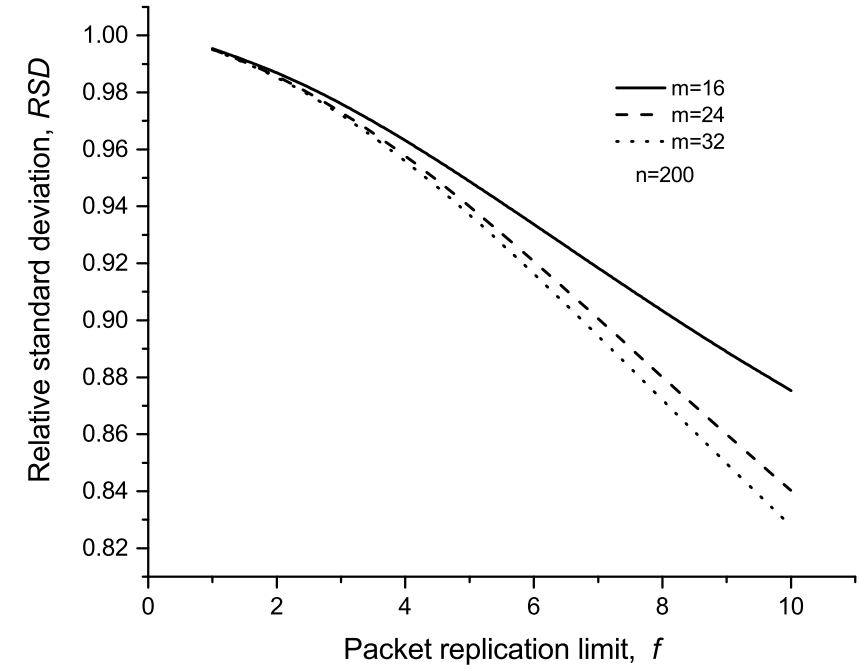

(b) RSD versus f in 2D MANET

Figure 5-6: The impact of packet redundancy limit f on packet delivery delay performance in 2D MANET

and medium contention issues begin to dominate the delivery performance, and thus the packet delivery delay increases. We can see from Figure 5-3 that the simulated results under the i.i.d. mobility model match nicely with the theoretical ones. This further validates our theoretical models.

We proceed to explore how the packet delivery delay varies with packet redundancy limit f. We can see from Figure 5-4 that the expected packet delivery delay decreases with f. This is because as f increases, there will be more relay nodes carry copies of the packet, the opportunity that destination node receives a packet will increase, and thus reducing the packet delivery delay. A further careful observation of Figure 5-4(a) indicates that for each setting of f, a bigger m could result in a bigger packet delivery delay. It can be explained as follows: we know that the considered network area is divided into m^3 cells and the mobile nodes roam from one cell to another, which results in the nodes sparsely distributed in the network as m increases, and thus the packet delivery delay increases. Different from that of the performance $E\{a_1\}$, we can see from Figure 5-4(b) that the behavior of RSD is very similar for all the settings of m. Figure 5-4 also shows that the simulated results under the i.i.d. mobility model match nicely with the theoretical ones.

5.3.4 Performance Comparison

In this subsection, we compare the packet delivery delay performance in 3D MANET with that in 2D MANET. Specifically, we choose a well-known cell-partitioned 2D MANET [78] and adopt two-hop relay algorithm for packet routing. The corresponding results in 2D MANET are summarized in Figures. 5-5 and 5-6.

For the same setting of these parameters in Figures. 5-3 and 5-5, and also in Figures. 5-4 and 5-6, these figures show that the expected packet delivery delay in 3D MANET is much bigger than that in 2D MANET. This phenomenon can be explained as follows. Recalling that in 3D MANET, the considered network area is evenly divided into m^3 cells, while in 2D MANET, the number of cells is m^2. Under the same setting of the number of nodes n, a larger value of the number of cells leads to a lower node density (i.e., n/the number of cells). Thus the nodes in 3D MANET is much

more sparsely distributed than those in 2D MANET. Since the packet delivery speed becomes lower in a more sparsely distributed network, the expected packet delivery delay in 3D MANET is much bigger than that in 2D MANET. It also demonstrates that the packet delivery delay performance in 3D MANET is different with that in 2D MANETs. Thus, it is proved that the packet delivery delay performance indeed requires to be analyzed differently for 3D MANETs.

5.4 Summary

In this chapter, we first develop a Markov chain theoretical framework to depict the packet delivery process under two-hop relay algorithm with packet redundancy. With the help of the Markov chain theoretical framework, we then derive analytical expressions for mean and relative standard deviation of packet delivery delay. Simulation results indicate that our theoretical models can accurately predict packet delivery delay performance in 3D MANETs. We compare the packet delivery delay performance in 3D MANET with that in 2D MANET. For the same network scenario, the expected delivery delay of 3D MANETs is bigger than that of 2D MANETs. This indicates that the analysis of the packet delivery delay performance in 3D MANETs is of great importance.

Chapter 6

Throughput Capacity Study in 3D MANETs

Throughput capacity is of great importance for the design and performance optimization of 3D MANETs. This chapter studies the exact throughput capacity of 3D MANETs under the routing algorithm introduced in chapter 3. Under this routing algorithm, each source node can transmitted a packet to at most f relay nodes, which forward the packet to its destination node. To study the throughput capacity of 3D MANETs, we first construct two absorbing Markov chain theoretical frameworks to depict the packet distributing process at source and the packet receiving process at destination. Based on these two theoretical frameworks, an analytical expression of the throughput capacity is further derived.

6.1 Performance Metric

Throughput capacity: For a 3D MANET with the considered 2HR-f algorithm, the per node throughput capacity (throughput capacity for brevity) is defined as the maximum value of input rate λ that the network can stably support.

6.2 Markov Chain Theoretical Frameworks and Throughput Capacity

6.2.1 Some Basic Transmission Probabilities

In order to derive the throughput capacity, we first analyze the transmissions may happen in considered 3D MANET, and then, we give some basic transmission probabilities. Their derivations are omitted here sice derivation processes are similar to these in Chapter 4. We present them here to help understanding.

Lemma 5. *Consider a given time slot and a tagged transmission flow, the probability that the source node S executes a Source-to-Destination transmission, it was denoted by p_{sd}. The probability that the S executes a Source-to-Relay or Relay-to-Destination transmission, it was denoted by p_{srd}. Then we have*

$$\begin{aligned} p_{sd}=&\frac{1}{\alpha^3}\Big\{\frac{27-m^3}{n-1}+\frac{m^3}{n}-\frac{26}{n-1}\Big(\frac{m^3-1}{m^3}\Big)^{n-1} \\ &+\Big(\frac{m^3}{n-1}-\frac{m^3}{n}\Big)\Big(\frac{m^3-1}{m^3}\Big)^{n}\Big\} \end{aligned} \tag{6.1}$$

$$\begin{aligned} p_{srd} = &\frac{m^3-27}{m^3\alpha^3}\Big\{\sum_{k=1}^{n-2}\binom{n-2}{k}\Big(\frac{1}{m^3}\Big)^k\Big(\frac{m^3-1}{m^3}\Big)^{n-2-k}\frac{1}{k+1} \\ &+\sum_{k=1}^{n-2}\binom{n-2}{k}\Big(\frac{26}{m^3}\Big)^k\Big(\frac{m^3-27}{m^3}\Big)^{n-2-k}\Big\} \end{aligned} \tag{6.2}$$

Lemma 6. *For a given time slot and a tagged transmission flow, suppose that source node S is sending the copy of the packet which in its send-queue, and the destination node is requesting for the same packet, continue to suppose that there are k copies of this packet in the network. We use $P_r(k)$ and $P_d(k)$ to denote the probability that D will receive the packet, the probability that S will successfully send a copy of the packet to a relay node which no carrying the packet, respectively, in the next time slot. Then*

we have

$$P_r(k) = p_{sd} + \frac{k-1}{2(n-2)} \cdot p_{srd} \tag{6.3}$$

$$P_d(k) = \frac{n-k-1}{2(n-2)} \cdot p_{srd} \tag{6.4}$$

6.2.2 Markov Chain Theoretical Frameworks

After deliberating over all possible transmissions in considered network model, in this section, two Markov chain theoretical frameworks are developed to trace the packet transmission process under two-hop relay scheme with packet redundancy, one is for analysing the packet service time at source node, the other is for analysing packet service time at destination node. Firstly, here we review the queues in source node and destination node and their operations, then introduce two service time mentioned before.

For a specified flow, the source S maintains a send-queue which stores the locally generated packets and operates as follows: once a local packet P is generated, the P is put to the end of the queue; once the copies dispatching for the head-of-line packet is done, S moves it out of the queue and moves ahead the remaining packets waiting behind it. The head-of-line packet of the send-queue indicates which packet the S is currently distributing copies for.

The destination D maintains a virtual queue which stores the *send numbers* of those packets not received yet by D, and the head-of-line entry presents the *send number* of the packet that the D is currently requesting for. The virtual queue operates as follows: once a packet P is moved to the head-of-line of the send-queue at S, the corresponding packet send number $SN(P)$ is put to the end of the virtual queue; every time the D receives a packet whose *send number* equals to the head-of-line entry, the D moves the head-of-line entry out of the virtual queue and moves ahead the remaining entries.

Now, we proceed to introduce the definitions of service time at source node and destination node,respectively.

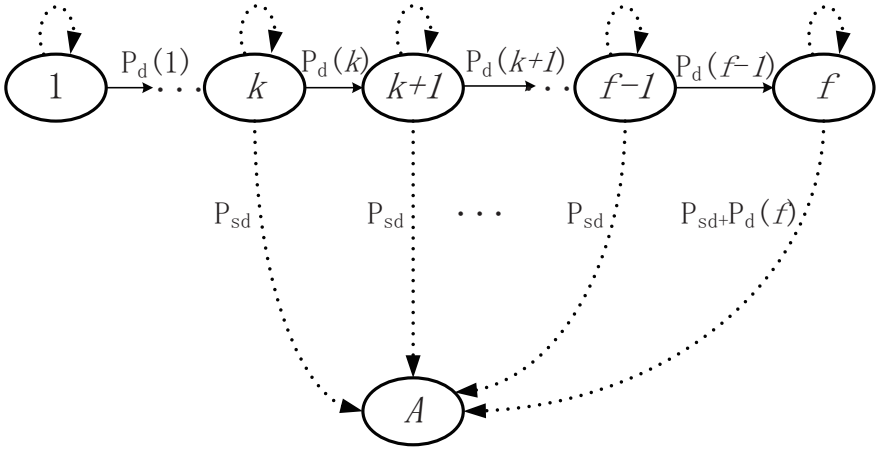

(a) Absorbing Markov chain for the packet transmitting process at the source node S.

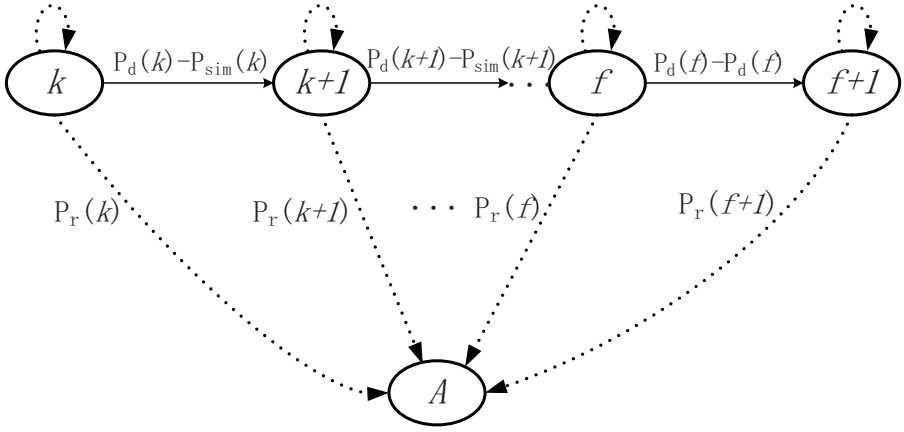

(b) Absorbing Markov chain for the packet reception process at the destination node D.

Figure 6-1: Absorbing Markov chains for packet P, given that the D starts to request for the P when there are already k copies of P in the network.

Definition 3. *For a packet P, the service time at the source S is the time elapsed between the time slot when the P was moved in the head-of-line at the send-queue source S and the time slot when the P was removed from send-queue source S.*

Definition 4. *For a packet P, the service time at the destination D is the time elapsed between the time slot when the D starts to request for the P and the time slot when the D receives the P.*

For a packet P, we assume there are 1 to k copies of P in the network when its destination D starts to request for the packet. If we use A to denote the absorbing

status for P, then the deliver processes for the packet at its source S and receive processes at its destination D can be defined by two finite-status absorbing Markov chains shown in Figure 6-1(a) and Figure 6-1(b), respectively. We use $X_S(k)$ and $X_D(k)$ to the denote the corresponding service time of packet P at the S and the D, respectively [1]. From the theory of Markov chain [74], we can see that the $X_S(k)$ can be regarded as the time the Markov chain in the Figure 6-1(a) takes to become absorbed given that the chain starts from the status 1, and the $X_D(k)$ can be regarded as the time the Markov chain in the Figure 6-1(b) takes to become absorbed given that the chain starts from the status k.

Lemma 7. *For a packet P of the tagged transmission flow, suppose that there are k copies of P in the network when the destination node D starts to request for the P, $1 \leq k \leq f+1$, then we have*

$$\mathbf{E}\{X_S(k)\} = \begin{cases} \sum_{i=1}^{k-1} \frac{1}{P_d(i)} + \frac{1}{p_{sd}+P_d(k)} \\ \qquad \cdot\big(1 + \sum_{j=1}^{f-k} \phi_2(k,j)\big) & \text{if } 1 \leq k \leq f, \\ \sum_{i=1}^{f} \frac{1}{P_d(i)} & \text{if } k = f+1. \end{cases} \tag{6.5}$$

$$\mathbf{E}\{X_D(k)\} = \begin{cases} \frac{1}{p_{sd}+p_{srd}/2}\big(1 + \sum_{j=1}^{f-k} \phi_3(k,j) \\ + \frac{P_d(f)}{P_r(f+1)}\phi_3(k,f-k)\big) & \text{if } 1 \leq k \leq f-1, \\ \frac{1}{p_{sd}+p_{srd}/2}\big(1 + \frac{P_d(f)}{P_r(f+1)}\big) & \text{if } k = f, \\ \frac{1}{P_r(f+1)} & \text{if } k = f+1. \end{cases} \tag{6.6}$$

where $\phi_2(k,j) = \prod_{t=1}^{j} \frac{P_d(k+t-1)}{p_{sd}+P_d(k+t)}$ *and* $\phi_3(k,j) = \prod_{t=1}^{j} \frac{P_d(k+t-1)}{p_{sd}+p_{srd}/2}$.

Proof: We derive (6.5) first. From the absorbing Markov chain in the Figure 6-1(a), if we use a_i to denote the expect time the Markov chain reaches absorbed status given that the chain starts from the status i, $1 \leq i \leq f$, and use q_{ij} to denote

[1] The $X_S(f+1)$ corresponds to the case that the D starts to request for the packet P from the status that there are $f+1$ copies in the network, i.e., f copies of P have been distributed.

the transition probability from status i to status j, $i, j \in [1, f]$, then we have

$$\mathbf{E}\{X_S(k)\} = a_1 \tag{6.7}$$

$$a_i = \frac{1 + \sum_{j\in[1,f],j\neq i} q_{ij} \cdot a_j}{1 - q_{ii}} \tag{6.8}$$

There will be three kinds of transfers in the Markov chain of the Figure 6-1(a), transfer back to itself, transfer to its next status (from status i to status $i+1$) and transfer to the absorbing status A. Thus, the a_i can be further determined as

$$a_i = \begin{cases} \frac{1}{P_d(i)} + a_{i+1} & \text{if } 1 \leq i < k, \\ \frac{1+P_d(i)\cdot a_{i+1}}{p_{sd}+P_d(i)} & \text{if } k \leq i < f, \\ \frac{1}{p_{sd}+P_d(f)} & \text{if } i = f. \end{cases} \tag{6.9}$$

The a_1 and thus the (6.5) can be derived from the (6.9) recursively.

Regarding the case that $k = f+1$, i.e., the destination D starts to request for the packet P after f copies of P have been transmitting to relays, it is easy to see that $\mathbf{E}\{X_S(f+1)\} = \sum_{i=1}^{f} \frac{1}{P_d(i)}$.

Now we proceed to derive (6.6). Similarly, for the Markov chain in the Figure 6-1(b), we have

$$\mathbf{E}\{X_D(i)\} = \begin{cases} \frac{1+P_d(i)\cdot\mathbf{E}\{X_D(i+1)\}}{p_{sd}+p_{srd}/2} & \text{if } k \leq i \leq f, \\ \frac{1}{P_r(f+1)} & \text{if } i = f+1. \end{cases} \tag{6.10}$$

The (6.6) can then be derived from the (6.10) recursively. ■

Lemma 8. *For any $1 \leq k \leq f$, we have*

$$\mathbf{E}\{X_S(k)\} < \mathbf{E}\{X_S(k+1)\} \tag{6.11}$$

$$\mathbf{E}\{X_D(k)\} > \mathbf{E}\{X_D(k+1)\} \tag{6.12}$$

Proof: We prove (6.11) first. When $k = f$,

$$\mathbf{E}\{X_S(f+1)\} - \mathbf{E}\{X_S(f)\} = \frac{1}{P_d(f)} - \frac{1}{p_{sd} + P_d(f)} > 0 \tag{6.13}$$

For the case that $1 \leq k < f$, according to (6.5) we have

$$\begin{aligned}
&\mathbf{E}\{X_S(k+1)\} - \mathbf{E}\{X_S(k)\} \\
&= \frac{1}{P_d(k)} + \frac{1}{p_{sd} + P_d(k+1)}\big(1 + \sum_{j=1}^{f-k-1} \phi_2(k+1, j)\big) \\
&\quad - \frac{1}{p_{sd} + P_d(k)}\big(1 + \sum_{j=1}^{f-k} \phi_2(k, j)\big) \\
&= \frac{1}{P_d(k)} + \frac{1}{p_{sd} + P_d(k+1)}\big(1 + \sum_{j=1}^{f-k-1} \phi_2(k+1, j)\big) \\
&\quad - \frac{1 + \frac{P_d(k)}{p_{sd}+P_d(k+1)}\big(1 + \sum_{j=1}^{f-k-1} \phi_2(k+1, j)\big)}{p_{sd} + P_d(k)} \qquad (6.14) \\
&= \frac{1}{P_d(k)} - \frac{1}{p_{sd} + P_d(k)} \\
&\quad + \frac{1 + \sum_{j=1}^{f-k-1} \phi_2(k+1, j)}{p_{sd} + P_d(k+1)}\big(1 - \frac{P_d(k)}{p_{sd} + P_d(k)}\big) \\
&> \frac{1}{P_d(k)} - \frac{1}{p_{sd} + P_d(k)} > 0 \qquad (6.15)
\end{aligned}$$

where the (6.14) follows after substituting

$$\sum_{j=1}^{f-k} \phi_2(k, j) = \frac{P_d(k)}{p_{sd} + P_d(k+1)}\big(1 + \sum_{j=1}^{f-k-1} \phi_2(k+1, j)\big).$$

Combining (6.13) and (6.15), the (6.11) follows.

Now we proceed to prove (6.12) using mathematical induction.

Initial step: when $k = f$, we have that

$$\begin{aligned}
\mathbf{E}\{X_D(f)\} &= \frac{1}{P_r(f+1)} \frac{P_d(f) + P_r(f+1)}{p_{sd} + \frac{p_{srd}}{2}} \\
&> \frac{1}{P_r(f+1)} = \mathbf{E}\{X_D(f+1)\} \qquad (6.16)
\end{aligned}$$

Inductive step: our inductive assumption is: there is a t, $1 < t \leq f$, such that $\mathbf{E}\{X_D(t)\} > \mathbf{E}\{X_D(t+1)\}$. We must prove the (6.12) is true for $k = t - 1$.

Since

$$\begin{aligned}
\mathbf{E}\{X_D(t-1)\} &= \frac{1 + P_d(t-1) \cdot \mathbf{E}\{X_D(t)\}}{P_d(t-1) + P_r(t-1)} \\
&> \frac{1 + P_d(t) \cdot \mathbf{E}\{X_D(t+1)\}}{P_d(t) + P_r(t)} \qquad (6.17) \\
&= \mathbf{E}\{X_D(t)\} \qquad (6.18)
\end{aligned}$$

where the (6.17) follows because $P_d(t) < P_d(t-1)$, $\mathbf{E}\{X_D(t+1)\} < \mathbf{E}\{X_D(t)\}$ and $P_d(t-1) + P_r(t-1) = P_d(t) + P_r(t)$. The (6.18) completes the inductive step.

■

Lemma 9. *For a 2HR-f 3D MANET, regarding the average service time at the source S taken over all locally generated packets, denote by X_S, the average service time at the destination D taken over all received packets, denote by X_D, we have*

$$X_S \leq X_D \qquad (6.19)$$

Since the X_S and X_D are taken over all locally generated packets and all received packets, respectively, together with the Lemma 8, we have

$$\mathbb{E}\{X_S(1)\} \leq X_S \leq \mathbb{E}\{X_S(f+1)\} \qquad (6.20)$$

$$\mathbb{E}\{X_D(f+1)\} \leq X_D \leq \mathbb{E}\{X_D(1)\} \qquad (6.21)$$

In light of the monotonicity property of $\mathbb{E}\{X_S(f+1)\}$ and $\mathbb{E}\{X_D(f+1)\}$, it is easy to see that we always have $\mathbb{E}\{X_S(f+1)\} \leq \mathbb{E}\{X_D(f+1)\}$. Then the Lemma 9 follows.

6.2.3 Throughput Capacity

In this section we derive per node throughput capacity.

Theorem 1. *For a 3D MANETs with the two-hop relay algorithm with packet redundancy, ($0 \leq f$), if we denote the per node throughput capacity by μ, then we have*

$$\mu = \begin{cases} p_{sd} + \frac{f}{2(n-2)} \cdot p_{srd} & \text{if } 1 \leq f, \\ p_{sd} & \text{if } f = 0. \end{cases} \tag{6.22}$$

Proof: As indicated in the Lemma 9 that we always have $X_S \leq X_D$, so the actual throughput for the tagged transmission flow is $1/X_D$. Then the per node (transmission flow) throughput capacity can be determined as

$$\begin{aligned} \mu &= \max\{1/X_D\} \\ &= \frac{1}{\mathbb{E}\{X_D(f+1)\}} && (6.23) \\ &= p_{sd} + \frac{f}{2(n-2)} \cdot p_{srd} && (6.24) \end{aligned}$$

where the (6.23) is due to (6.21) and the (6.24) is due to (6.6).

Regarding the case that $f = 0$, since only the Procedure 1, i.e., the source-to-destination transmission, will be executed, it is easy to see that $\mu = p_{sd}$. ■

6.3 Numerical Results

In this section, we first provide simulation results to validate the efficiency of our theoretical expression on throughput capacity, and then apply it to investigate how system parameters will affect the throughput capacity under the considered routing algorithm.

6.3.1 Validation of Throughput Capacity

We develop a simulator to simulate the packet delivery process of the considered routing algorithm in the considered MANETs. Here, the parameter in scheduling is determined as α=min$\{9, m\}$ with the setting of the guard zone $\Delta = 1$. In addition to the i.i.d. mobility model, the random walk model [68] and random waypoint

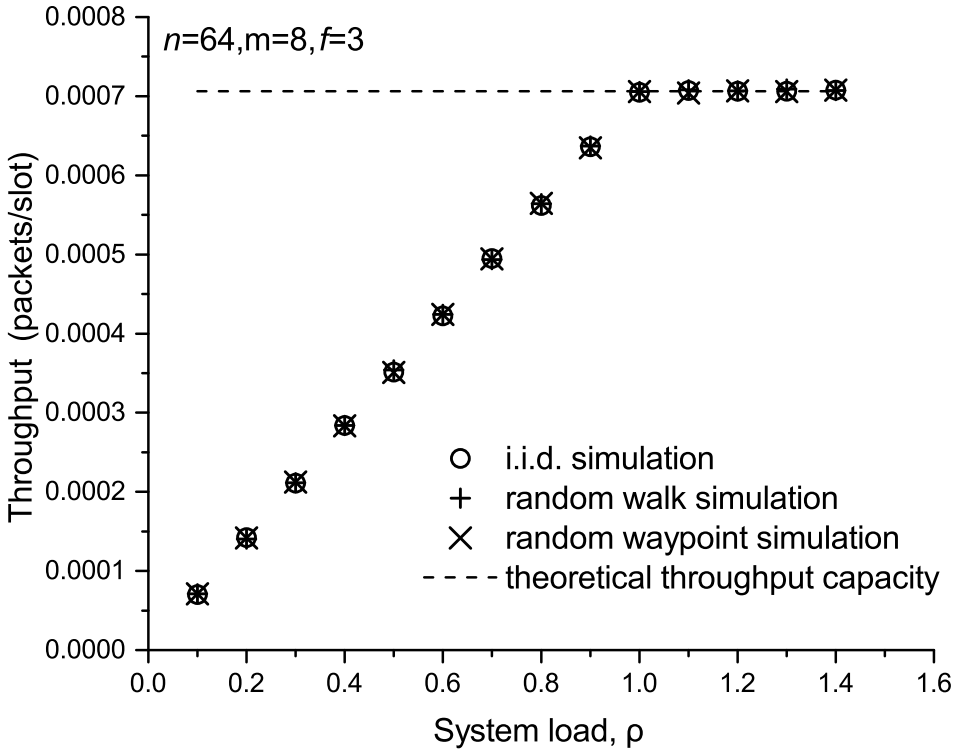

Figure 6-2: The per node throughput for network scenario ($n = 64, m = 8, f = 3$.)

model [77], are also implemented in the simulator.Based on the simulator, extensive simulations were conducted to verify the theoretical expression on throughput capacity under the network scenarios of $n = 64, m = 8, f = 3$. The simulation results on throughput under different system loads ρ ($\rho = \lambda/\mu$) are summarized in Figure 6-2, where the throughput is measured as the time average of number of packets that are successfully delivered from a source node to its destination node. As shown in Figure 6-2, each simulation result on throughput is averaged over 10^6 time slots for each given system load ρ, and the dots represent the simulated throughput and the dashed lines are the corresponding theoretical throughput capacity μ, calculated by Theorem 1.

Figure 6-2 shows that the per node throughput first increases linearly with ρ till the input rate λ increases to the value no less than the theoretical throughput

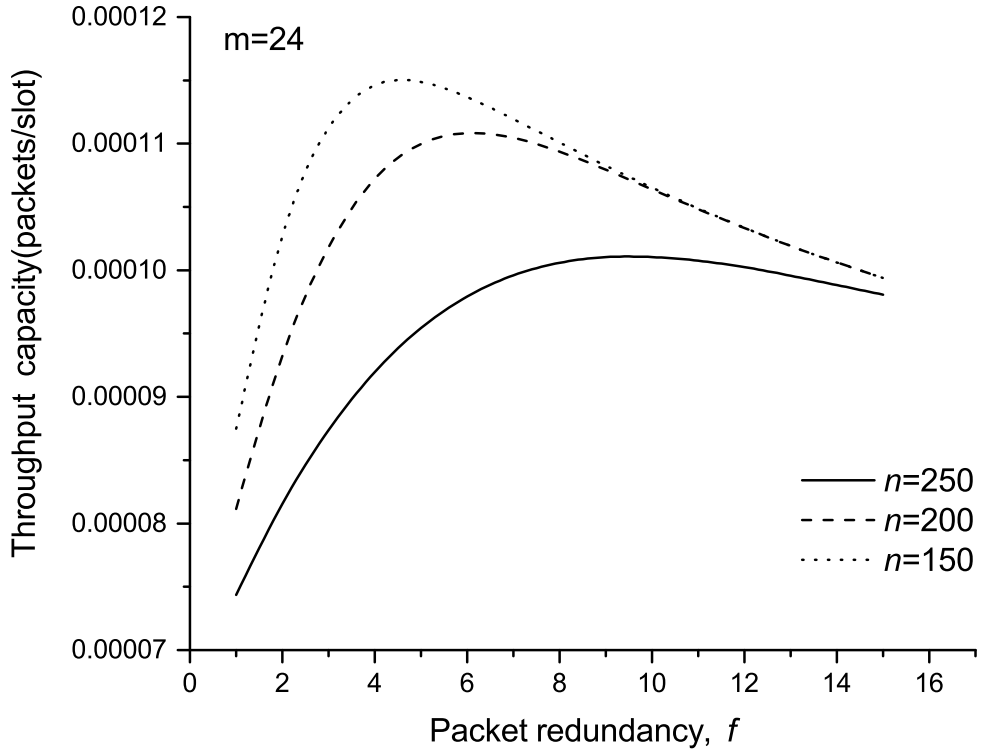

Figure 6-3: Throughput capacity μ versus packet redundancy f

capacity μ, the per node throughput will achieve theoretical throughput capacity μ of 7.0×10^{-4} in Figure 6-2.

Another observation from Figure 6-2 is that the throughput under the random walk or random waypoint model also achieves the throughput capacity developed based on the i.i.d. mobility model. It suggests that our throughput capacity result can also be used to estimate the throughput capacity for these mobility models. It also implies that the throughput capacity depends only on the nodes locations. Since both of these mobility models lead to a uniform distribution of nodes locations , they lead to an identical throughput capacity to that of the i.i.d. mobility model.

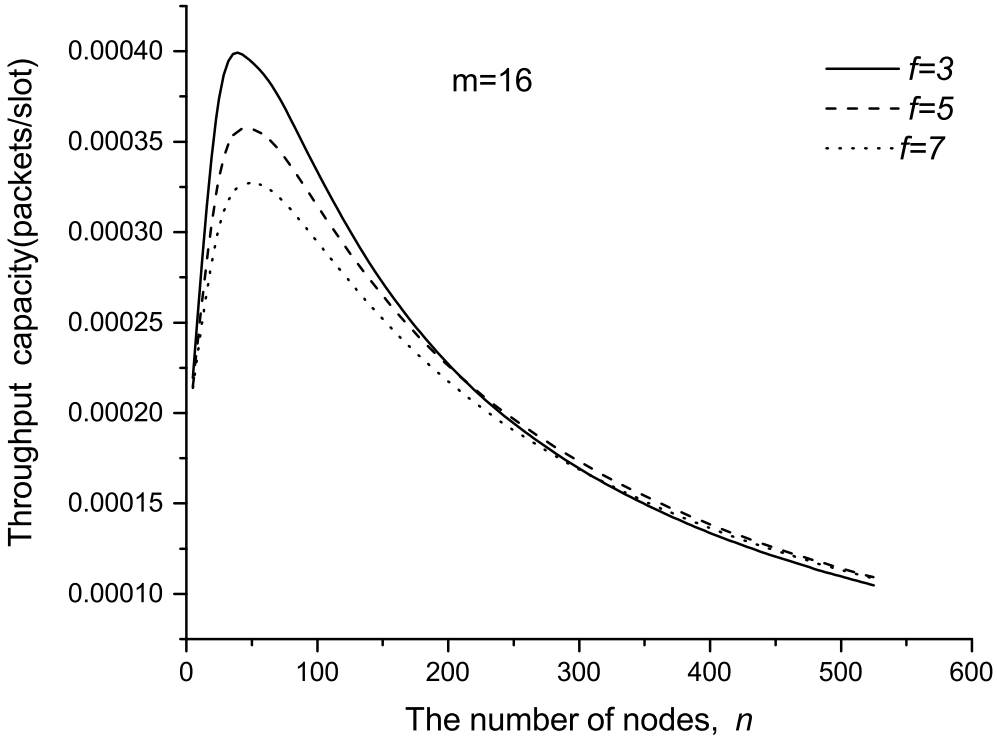

Figure 6-4: Throughput capacity μ versus number of nodes n.

6.3.2 Impact of System Parameters on Throughput Capacity

Firstly, we explore the impact of the parameter f on the throughput capacity. For given $m = 24$, when $n = 250$, $n = 200$, $n = 150$, respectively, the per node throughput capacity μ vs. the packet redundancy f are summarize in Figure 6-3.

From Figure 6-3 we can see that for each setting of f, the throughput capacity first increases and then decreases as f increases. This is due to the following reasons: increase of f has a two-fold effect on the throughput capacity. On the one hand, when f is small, increasing f namely increasing the relay nodes, thus destination node get more opportunities to receive the packet from relay nodes, as a result, increase f increases throughput capacity; on the other hand, when f becomes larger, increasing f may increase the delivery time for a packet and thus decreases throughput capacity.

Finally, we explore in Figure 6-4 how the throughput capacity varies with the num-

ber of nodes n, given that $m = 16$ and $f = \{3, 5, 7\}$. We can observe from Figure 6-4 that for each setting of f, as n increases, the throughput capacity first increases and then decreases. This can be explained as follows: on one hand, when the network is sparse (thus n is relatively small), increasing n will result in more opportunities for source or relays to execute transmissions and thus increases throughput capacity; however, on the other hand, a larger n will cause more significant interferences and medium contentions among nodes and thus results in a decrease of transmission opportunities for each node, and incurs the decrease of throughput capacity.

6.4 Summary

In this chapter, we investigated the per node throughput capacity of 3D MANETs under the considered routing algorithm. Two absorbing Markov chain frameworks were constructed to depict the packet distributing processes at source and destination, respectively. With the help of the Markov chain frameworks, an analytical expression of throughput capacity was derived. Extensive simulation illustrates that the analytical expression can accurately capture the throughput capacity under the considered routing. In addition, the impacts of the number of nodes and the packet redundancy on throughput capacity are discussed in this chapter.

THIS PAGE INTENTIONALLY LEFT BLANK

Chapter 7

Conclusion

This chapter summarizes our contributions and points out future research directions.

7.1 Summary of the Thesis

This work focuses on the performance studies for 3D MANETs with two-hop relay algorithm with packet redundancy. The main contributions are summarized as follows.

- By combining two-hop relay and packet redundancy techniques, we developed a general two-hop relay algorithm with packet redundancy to the study of packet delivery probability performance in 3D MANETs under permutation traffic pattern. We then developed a Markov chain theoretical framework to model packet delivery process under the routing algorithm. With the help of the theoretical framework, we further derived the analytical expressions for the packet delivery probability. In addition, the lifetime of packet delivery was considered in studying packet delivery probability, i.e., we can obtain delivery probability result under any given packet lifetime, it is meaningful to network designer. Moreover, the impacts of network parameters such as redundancy limit f, the number of nodes n, on the packet delivery probability were analysed.

- We studied packet delivery delay performance in 3D MANETs under two-hop

relay algorithm with packet redundancy. We developed a Markov chain theoretical framework to model packet delivery process under the routing algorithm, based on which we then derived the analytical expressions for both the mean and variance of packet delivery delay in 3D MANETs, where the interference and medium access control are taken into account. We validated the theoretical framework under i.i.d. mobility model, random walk model and random waypoint model, the results show that although the theoretical framework was developed under i.i.d. mobility model, it can also apply to random walk and random waypoint model. Theoretical results indicated that packet redundancy technique can remarkably decrease packet delay and delay variance. It is expected that our study can provide an efficient support for these critical applications with stringent delay/variance requirements in future 3D MANETs.

- Finally, we investigated the throughput capacity of 3D MANETs under the above proposed routing algorithm. We developed two absorbing Markov chain theoretical frameworks to depict the packet distributing/receiving processes at source and destination, respectively. Based on these two Markov chain theoretical frameworks, via deriving the service time at source node and service time at destination node, we further derived an analytical expression for throughput capacity. We also discussed how the packet redundancy and the number of nodes affect the throughput capacity.

7.2 Future Works

We summarize the future interesting directions as follows.

- In this thesis, we adopt unicast for packet dispatching. As discussed above, the nodes density in 3D MANETs is sparser than that in 2D MANETs, therefore, one interesting future direction is to further explore the performance of 3D MANETs under a more efficient packet dispatching way, e.g. broadcast.

- We developed Markov chain-based theoretical frameworks to explore packet de-

livery performance in cell-partitioned 3D MANETs, and it will be an interesting direction to study how to evaluate the performance under our theoretical frameworks in other network scenarios, such as delay tolerant networks (DTNs) [81] and ALOHA networks [82].

- It is notable that our studies in this thesis focused on two-hop relay 3D MANETs. Another interesting direction is to further extend the developed theoretical models to analyze packet delivery performance in multi-hop relay 3D MANETs. It is also interesting to explore the network performance with the consideration of constraints of nodes buffer size and packet loss in our future research.

THIS PAGE INTENTIONALLY LEFT BLANK

Appendix A

Proofs of the Lemmas 1-2

Proof of Lemma 1:. The source node S conducts a Source-to-Destination transmission if the following three events happen simultaneously: S is in an active cell, S is selected as the transmitter, and the node D is either in the same cell with S or in one adjacent cell of S. The third event includes following two mutually exclusive cases: both S and D are inside this cell; or the S is inside this cell while the D is inside one of the 26 adjacent cells of this cell. We assume that apart from the nodes S and D, there are k other nodes inside this cell, $k \in [0, n-2]$, the probability that the node S is selected as the transmitter is $\frac{1}{k+2}$ (resp. $\frac{1}{k+1}$) under the former case (resp. under the latter case). Summing up the probabilities under these two cases,

then we have

$$
\begin{aligned}
p_{sd} = \frac{1}{\alpha^3}\Bigg\{ & \sum_{k=0}^{n-2}\binom{n-2}{k}\Big(\frac{1}{m^3}\Big)^k\Big(\frac{m^3-1}{m^3}\Big)^{n-2-k}\frac{1}{m^3}\frac{1}{k+2} \\
& +\sum_{k=0}^{n-2}\binom{n-2}{k}\Big(\frac{1}{m^3}\Big)^k\Big(\frac{m^3-1}{m^3}\Big)^{n-2-k}\frac{26}{m^3}\frac{1}{k+1}\Bigg\} \\
= \frac{1}{\alpha^3}\Bigg\{ & \sum_{k=0}^{n-2}\binom{n-1}{k+1}\Big(\frac{1}{m^3}\Big)^{k+1}\Big(\frac{m^3-1}{m^3}\Big)^{n-2-k}\frac{1}{k+2} \\
& -\sum_{k=0}^{n-2}\binom{n-2}{k+1}\Big(\frac{1}{m^3}\Big)^{k+1}\Big(\frac{m^3-1}{m^3}\Big)^{n-2-k}\frac{1}{k+2} \\
& +\sum_{k=0}^{n-2}\binom{n-2}{k}\Big(\frac{1}{m^3}\Big)^{k+1}\Big(\frac{m^3-1}{m^3}\Big)^{n-2-k}\frac{26}{k+1}\Bigg\} \\
= \frac{1}{\alpha^3}\Bigg\{ & \frac{27-m^3}{n-1}+\frac{m^3}{n}-\frac{26}{n-1}\Big(\frac{m^3-1}{m^3}\Big)^{n-1} \\
& +\Big(\frac{m^3}{n-1}-\frac{m^3}{n}\Big)\Big(\frac{m^3-1}{m^3}\Big)^{n}\Bigg\}
\end{aligned}
\tag{A.1}
$$

Notice that $\binom{n}{r}=\binom{n+1}{r+1}-\binom{n}{r+1}$ and $\frac{1}{r+1}\binom{n}{r}=\frac{1}{n+1}\binom{n+1}{r+1}$. So the formula (4.1) follows.

Similarly, the S conducts a Source-to-Relay or Relay-to-Destination transmission if the following four events happen concurrently: S is in an active cell, S is selected as the transmitter, there is at least one other node (except S and D) in the same cell of S or its 26 adjacent cells, and the node D is in one of the other m^3-27 cells(excluding this cell and its 26 adjacent cells). The probability that the D is in one of the other m^3-27 cells is $\frac{m^3-27}{m^3}$. The third event includes the following two mutually exclusive cases: this cell contains only node S; or this cell contains at least one other node aside from node S. If we suppose that there are k ($k\in[1,n-2]$) other nodes inside this cell (resp. the 26 adjacent cells of this cell), then the other $n-2-k$ nodes can be in any cell of the other m^3-1 (resp. m^3-27) cells. Summing up the probabilities under these two cases, then we have

$$
\begin{aligned}
p_{srd} = \frac{m^3-27}{m^3\alpha^3}\Bigg\{ & \sum_{k=1}^{n-2}\binom{n-2}{k}\Big(\frac{1}{m^3}\Big)^k\Big(\frac{m^3-1}{m^3}\Big)^{n-2-k}\frac{1}{k+1} \\
& +\sum_{k=1}^{n-2}\binom{n-2}{k}\Big(\frac{26}{m^3}\Big)^k\Big(\frac{m^3-27}{m^3}\Big)^{n-2-k}\Bigg\}
\end{aligned}
\tag{A.2}
$$

Proof of Lemma 2: In the next time slot, the destination node D may receive a packet either from the source node S or from one of the $g-1$ relay nodes. Notice that these events are mutually exclusive, the probability that D receives a packet from S is p_{sd}, and the probability that D receives a packet from a single relay node is $\frac{p_{srd}}{2(n-2)}$. By summing up the probabilities of these events, the formula (4.4) follows. Similarly, in the next time slot the node S may transmit out a packet to any one of relay nodes. Notice that these events are also exclusive, and the probability that S transmits out a packet to a single relay node is $\frac{p_{srd}}{2(n-2)}$, so the formula (4.3) follows.

To derive $P_{sim}(g)$, let's focus on a specific relay node R which carries a copy of the packet and a specific relay node V which does not carry any copy of the packet. We use $P(S \to V, R \to D)$ to denote the probability that a Source-to-Relay transmission from S to V and a Relay-to-Destination transmission from R to D happen simultaneously in the next time slot. Thus the $P_{sim}(g)$ can be determined as

$$P_{sim}(g) = P(S \to V, R \to D) \tag{A.3}$$

First, we consider the active cell with node R. The R can conduct a Relay-to-Destination transmission with D only under the following two mutually exclusive cases: D is in this cell or D is in one of the 26 adjacent cells. We suppose that except the S, D, R, V, and the destination node of R's local traffic, there are in total k other nodes in the one-hop neighborhood of R, $k \in [0, n-5]$, among them i nodes are in the same cell as R, $i \in [0, k]$, and the other $k-i$ nodes are in the 26 adjacent cells. Then the probability that R and D are selected as the transmitter and the receiver, respectively, is $\frac{1}{(i+2)(k+1)}$ (resp. $\frac{1}{(i+1)(k+1)}$) under the former case (resp. under the latter case). Summing up the probabilities under these two cases, then we get the corresponding probability of the Relay-to-Destination transmission $R \to D$. Similarly, we can also get the probability of the Source-to-Relay transmission $S \to V$. Multiplying two probabilities corresponding to Source-to-Relay and Relay-

to-Destination transmission, and then we have

$$
\begin{aligned}
P_{sim}(g) &= \frac{(g-1)(n-g-1)(m^3-\alpha^3)}{4m^3\alpha^6}\sum_{k=0}^{n-5}\binom{n-5}{k} \\
&\cdot\Big(\sum_{i=0}^{k}\binom{k}{i}\frac{1}{k+1}\Big(\frac{1}{i+2}+\frac{26}{i+1}\Big)\Big(\frac{1}{m^3}\Big)^{i+1}\Big(\frac{26}{m^3}\Big)^{k-i}\Big) \\
&\cdot\sum_{t=0}^{n-4-k}\binom{n-4-k}{t}\Big(\sum_{l=0}^{t}\binom{t}{l}\frac{1}{t+1}\Big(\frac{1}{l+2}+\frac{26}{l+1}\Big) \\
&\Big(\frac{1}{m^3}\Big)^{l+1}\Big(\frac{26}{m^3}\Big)^{t-l}\Big)\Big(\frac{m^3-54}{m^3}\Big)^{n-4-k-t}
\end{aligned}
\tag{A.4}
$$

Notice that

$$
\begin{aligned}
&\sum_{i=0}^{k}\binom{k}{i}\frac{1}{k+1}\Big(\frac{1}{i+2}+\frac{26}{i+1}\Big)\Big(\frac{1}{m^3}\Big)^{i+1}\Big(\frac{26}{m^3}\Big)^{k-i}\Big) \\
&=\sum_{i=0}^{k}\binom{k+1}{i+1}\frac{1}{k+1}\frac{1}{i+2}\Big(\frac{1}{m^3}\Big)^{i+1}\Big(\frac{26}{m^3}\Big)^{k-i} \\
&\quad-\sum_{i=0}^{k}\binom{k}{i+1}\frac{1}{k+1}\frac{1}{i+2}\Big(\frac{1}{m^3}\Big)^{i+1}\Big(\frac{26}{m^3}\Big)^{k-i} \\
&\quad+\sum_{i=0}^{k}\binom{k}{i}\frac{1}{k+1}\frac{26}{i+1}\Big(\frac{1}{m^3}\Big)^{i+1}\Big(\frac{26}{m^3}\Big)^{k-i} \\
&=\frac{1}{(k+1)(k+2)}\Big\{27\Big(\frac{27}{m^3}\Big)^{k+1}-(k+10)\Big(\frac{26}{m^3}\Big)^{k+1}\Big\} \\
&\quad-\frac{1}{(k+1)^2}\Big\{26\Big(\frac{27}{m^3}\Big)^{k+1}-(k+9)\Big(\frac{26}{m^3}\Big)^{k+1}\Big\} \\
&\quad+\frac{26}{(k+1)^2}\Big\{\Big(\frac{27}{m^3}\Big)^{k+1}-\Big(\frac{26}{m^3}\Big)^{k+1}\Big\} \\
&=\frac{27(\frac{27}{m^3})^{k+1}-26(\frac{26}{m^3})^{k+1}}{(k+1)(k+2)}
\end{aligned}
\tag{A.5}
$$

□

Bibliography

[1] J. Andrews, S. Shakkottai, R. Heath, N. Jindal, M. Haenggi, R. Berry, D. Guo, M. Neely, S. Weber, S. Jafar, and A. Yener. Rethinking information theory for mobile ad hoc networks. *IEEE Commun. Mag.*, 46(12):94–101, Dec. 2008.

[2] I.F. Akyildiz and E.P. Stuntebeck. Wireless underground sensor networks: Research challenges. *Ad Hoc Networks*, 4(6):669–686, 2006.

[3] X. Dong and M.C. Vuran. Spatio-temporal soil moisture measurement with wireless underground sensor networks. In *Ad Hoc Networking Workshop (Med-Hoc-Net), 2010 The 9th IFIP Annual Mediterranean*, pages 1–8. IEEE, 2010.

[4] Y. Wang, S. Jain, M. Martonosi, and K. Fall. Erasure-coding based routing for opportunistic networks. In *WDTN*, 2005.

[5] Y. Liao, K. Tan, Z. Zhang, and L. Gao. Estimation based erasure coding routing in delay tolerant networks. In *IWCMC*, 2006.

[6] L. Chen, C. Yu, T. Sun, Y. Chen, and H. Chu. A hybrid routing approach for opportunistic networks. In *ACM SIGCOMM.*, 2006.

[7] A. A. Hanbali, A. A. Kherani, and P. Nain. Simple models for the performance evaluation of a class of two-hop relay protocols. In *IFIP Netw.*, 2007.

[8] F. Tsapeli and V. Tsaoussidis. Routing for opportunistic networks based on probabilistic erasure coding. In *WWIC*, 2012.

[9] J. Liu, X. Jiang, H. Nishiyama, and N. Kato. Performance modeling for two-hop relay with erasure coding in MANETs. In *Globecom*, 2011.

[10] M. J. Neely and E. Modiano. Capacity and delay tradeoffs for ad-hoc mobile networks. *IEEE Transactions on Information Theory*, 51(6):1917–1936, Jun. 2005.

[11] A. Panagakis, A. Vaios, and I. Stavrakakis. Study of two-hop message spreading in DTNs. In *WiOpt*, 2007.

[12] E. Bulut, Z. Wang, and B. K. Szymanski. cost effective multi-period spraying for routing in delay tolerant networks. *IEEE/ACM Trans. Netw.*, 18(5):1530–1543, Oct. 2010.

[13] J. Liu, X. Jiang, H. Nishiyama, and N. Kato. Delay and capacity in ad hoc mobile networks with f-cast relay algorithms. In *ICC*, 2011.

[14] J. Liu, X. Jiang, H. Nishiyama, and N. Kato. Generalized two-hop relay for flexible delay control in MANETs. *IEEE/ACM Trans. Netw.*, 20(6):1950–1963, Dec. 2013.

[15] P. Gupta and P.R. Kumar. The capacity of wireless networks. *IEEE Trans. Inf. Theory*, 46(2):388–404, Mar. 2000.

[16] B. Kannhavong, H. Nakayama, N. Kato, A. Jamalipour, and Y. Nemoto. A study of a routing attack in olsr-based mobile ad hoc networks. *International J. Communication Systems*, 20(11):1245–1261, Nov. 2007.

[17] B. Kannhavong, H. Nakayama, Y. Nemoto, N. Kato, and A. Jamalipour. A survey of routing attacks in mobile ad hoc networks. *IEEE Wirel. Commun. Mag.*, 14(5):85–91, Oct. 2007.

[18] C. Buraagohain, S. Suri, C. Toth, and Y. Zhou. Improved throughput bounds for interference-aware routing in wireless networks. In *COCOON*, 2007.

[19] O. Dousse, M. Franceschetti, and P. Thiran. On the throughput scaling of wireless relay networks. *IEEE Trans. Inf. Theory*, 52(6):2756–2761, Jun. 2006.

[20] M. Franceschetti, O. Dousse, D. N. C. Tse, and P. Thiran. Closing the gap in the capacity of wireless networks via percolation theory. *IEEE Trans. Inf. Theory*, 53(3):1009–1018, Mar. 2007.

[21] X. Lin, G. Sharma, and R. R. Mazumdarand N. B. Shroff. Degenerate delay-capacity tradeoffs in ad-hoc networks with brownian mobility. *IEEE/ACM Trans. Netw.*, 14(SI):2777C–2784, Jun. 2006.

[22] P. Li, Y. Fang, J. Li, and X. Huang. Smooth trade-offs between throughput and delay in mobile ad hoc networks. *IEEE Trans. Mobile Comput.*, 11(3):427–438, Mar. 2012.

[23] Y. Wang, X. Chu, X. Wang, and Y. Cheng. Throughput, delay, and mobility in wireless ad hoc networks. In *INFOCOM*, 2010.

[24] A. Panagakis, A. Vaios, and I. Stavrakakis. Study of two-hop message spreading in dtns. In *Modeling and Optimization in Mobile, Ad Hoc and Wireless Networks and Workshops, 2007. WiOpt 2007. 5th International Symposium on*, pages 1–8. IEEE, 2007.

[25] J. Whitbeck, V. Conan, and M. D. de Amorim. Performance of opportunistic epidemic routing on edge-markovian dynamic graphs. *IEEE Transactions on communications*, 59(5):1259–1263, 2011.

[26] A. Krifa, C. Barakat, and T. Spyropoulos. Message drop and scheduling in dtns: Theory and practice. *Mobile Computing, IEEE Transactions on*, 11(9):1470–1483, 2012.

[27] E. Altman, T. Başar, and P.F. De. Optimal monotone forwarding policies in delay tolerant mobile ad-hoc networks. *Performance Evaluation*, 67(4):299–317, 2010.

[28] E. Altman and F. D. Pellegrini. Forward correction and fountain codes in delay-tolerant networks. *Networking, IEEE/ACM Transactions on*, 19(1):1–13, 2011.

[29] W. Chahin, R. El-Azouz, Francesco D. P., and A. P. Azad. Blind online optimal forwarding in heterogeneous delay tolerant networks. In *Wireless Days (WD), 2011 IFIP*, pages 1–6. IEEE, 2011.

[30] R. El-Azouzi, F. De Pellegrini, H. B. Sidi, and V. Kamble. Evolutionary forwarding games in delay tolerant networks: Equilibria, mechanism design and stochastic approximation. *Computer Networks*, 57(4):1003–1018, 2013.

[31] J. Liu, X. Jiang, H. Nishiyama, and N. Kato. Delay and capacity in ad hoc mobile networks with f-cast relay algorithms. *IEEE Transactions on Wireless Communications*, 10(8):2738–2751, 2011.

[32] A. A. Hanbali, P. Nain, and E. Altman. Performance of ad hoc networks with two-hop relay routing and limited packet lifetime. In *Proceedings of the 1st international conference on Performance evaluation methodolgies and tools*, page 49. ACM, 2006.

[33] K. Wei, S. Guo, D. Zeng, K. Xu, and K. Li. Exploiting small world properties for message forwarding in delay tolerant networks. *IEEE Transactions on Computers*, 64(10):2809–2818, 2015.

[34] D. Moraes, M. Renato, H. R. Sadjadpour, and J.J. Garcia-Luna-Aceves. Reducing delay while maintaining capacity in mobile ad-hoc networks using multiple random routes. In *Signals, Systems and Computers, 2004. Conference Record of the Thirty-Eighth Asilomar Conference on*, volume 2, pages 1478–1482. IEEE, 2004.

[35] E. G. Abbas, M. James, P. Balaji, and S. Devavrat. Optimal throughput-delay scaling in wireless networks-part i: The fluid model. *IEEE Transactions on Information Theory*, 52(6):2568–2592, Jun. 2006.

[36] M. James and S. Devavrat. Throughput and delay in random wireless networks with restricted mobility. *IEEE Transactions on Information Theory*, 53(3):1108–1116, Mar. 2007.

[37] X. Lin, G. Sharma, R. R. Mazumdar, and N. B. Shroff. Degenerate delay-capacity tradeoffs in ad-hoc networks with brownian mobility. *IEEE/ACM*

Transactions on Networking, Special Issue on Networking and Information Theory, 52(6):2777–2784, Jun. 2006.

[38] G. Sharma, R. Mazumdar, and B. N. Shroff. Delay and capacity trade-offs for mobile ad hoc networks: A global perspective. *IEEE/ACM Transactions on Networking*, 15(5):981–992, Oct. 2007.

[39] T. Spyropoulos, K. Psounis, and C. S. Raghavendra. Spray and wait: An efficient routing scheme for intermittently connected mobile networks. In *ACM SIGCOMM Workshop*, 2005.

[40] J. Miao, O. Hasan, S. B. Mokhtar, L. Brunie, and G. Gianini. A delay and cost balancing protocol for message routing in mobile delay tolerant networks. *Ad Hoc Networks*, 25:430–443, 2015.

[41] G. Robin, N. Philippe, and K. Ger. The message delay in mobile ad hoc networks. *Performance Evaluation*, 62(1):210–228, Jul. 2005.

[42] X. Zhang, G. Neglia, K. Jim, and T. Don. Performance modeling of epidemic routing. *Computer Networks*, 51(10):2867–2891, Jul. 2007.

[43] A. H. Ahmad, N. Philippe, and A. Eitan. Performance of ad hoc networks with two-hop relay routing and limited packet lifetime (extended version). *Performance Evaluation*, 65(6):463–483, Dec. 2008.

[44] D. Knuth. *The Art of Computer Programming*. Addison-Wesley, 1998.

[45] M. Grossglauser and D. N. Tse. Mobility increases the capacity of ad hoc wireless networks. In *INFOCOM*, 2001.

[46] A. E. Gamal, J. Mammen, B. Prabhakar, and D. Shah. Throughput delay trade-off in wireless networks. In *INFOCOM*, 2004.

[47] J. Mammen and D. Shah. Throughput and delay in random wireless networks with restricted mobility. *IEEE Trans. Inf. Theory*, 53(3):1108C–1116, Mar. 2007.

[48] Y. Cai, X. Wang, Z. Li, and Y. Fang. Delay and capacity in MANETs under random walk mobility model. *Wirel. Netw.*, 20(3):525–536, Apr. 2014.

[49] R. Urgaonkar and M. J. Neely. Network capacity region and minimum energy function for a delay-tolerant mobile ad hoc network. *IEEE/ACM Trans. Netw.*, 19(4):1137C–1150, Aug. 2011.

[50] J. Gao, J.Liu, X. Jiang, O. Takahashi, and N. Shiratori. Throughput capacity of MANETs with group-based scheduling and general transmission range. *IEICE Trans. Commun.*, E96-B(7):1791–1802, Jul. 2013.

[51] J. Liu, X. Jiang, H. Nishiyama, and N. Kato. Delay and capacity in ad hoc mobile networks with f-cast relay algorithms. *IEEE Trans. Wirel. Commun.*, 10(8):2738–2751, Aug. 2011.

[52] P. Gupta, P. R. Kumar, et al. Internets in the sky: The capacity of three dimensional wireless networks. *Communications in Information and Systems*, 1(1):33–49, 2001.

[53] Li. P., M. Pan, and Fang. Y. Capacity bounds of three-dimensional wireless ad hoc networks. *Networking IEEE/ACM Transactions on*, 20(4):1304–1315, Aug. 2012.

[54] S. Durocher, D. Kirkpatrick, and L. Narayanan. On routing with guaranteed delivery in three-dimensional ad hoc wireless networks. *Wireless Networks*, 16(1):227–235, 2010.

[55] A. I. Alshabtat, L. Dong, J. Li, and F. Yang. Low latency routing algorithm for unmanned aerial vehicles ad-hoc networks. *International Journal of Electrical and Computer Engineering*, 6(1):48–54, 2010.

[56] Y. He, X. Cai, Y. Zhang, X. Han, Q. Lin, and Ch. Li. Routing protocol for complex three-dimensional vehicular ad hoc networks. In *Connected Vehicles and Expo (ICCVE), 2014 International Conference on*, pages 739–744. IEEE, 2014.

[57] Y. Wang. Three-dimensional wireless sensor networks: geometric approaches for topology and routing design. In *The Art of Wireless Sensor Networks*, pages 367–409. Springer, 2014.

[58] A. Y. Teymorian, W. Cheng, L. Ma, X. Cheng, X. Lu, and Z. Lu. 3d underwater sensor network localization. *IEEE Transactions on Mobile Computing*, 8(12), 2009.

[59] Q. Lin, C. Li, X. Wang, and L. Zhu. A three-dimensional scenario oriented routing protocol in vehicular ad hoc networks. In *Vehicular Technology Conference (VTC Spring), 2013 IEEE 77th*, pages 1–5. IEEE, 2013.

[60] S. Durocher, D. Kirkpatrick, and L. Narayanan. On routing with guaranteed delivery in three-dimensional ad hoc wireless networks. In *International Conference on Distributed Computing and Networking*, pages 546–557. Springer, 2008.

[61] L. Ying, S. Yang, and R. Srikant. Optimal delay-throughput trade-offs in mobile ad-hoc networks. *IEEE Trans. Inf. Theory*, 54(9):4119–4143, Sep. 2008.

[62] C. Zhang, Y. Fang, and X. Zhu. Throughput-delay tradeoffs in large-scale MANETs with network coding. In *INFOCOM*, 2009.

[63] Z. Kong, E. M. Yeh, and E. Soljanin. Coding improves the throughput-delay tradeoff in mobile wireless networks. *IEEE Trans. Inf. Theory*, 58(11):6894–6906, Nov. 2012.

[64] X. Wang, W. Huang, S. Wang, J. Zhang, and C. Hu. Delay and capacity tradeoff analysis for motioncast. *IEEE/ACM Trans. Netw.*, 19(5):1354–1367, Oct. 2011.

[65] S. R. Kulkarni and P. Viswanath. A deterministic approach to throughput scaling in wireless networks. *IEEE Trans. Inf. Theory*, 50(6):1041C1049, Jun. 2004.

[66] P. Gupta and P.R. Kumar. The capacity of wireless networks. *IEEE Transactions on Information Theory*, 46(2):388–404, Mar. 2000.

[67] M. Grossglauser and D. N. Tse. Mobility increases the capacity of ad hoc wireless networks. *IEEE/ACM Transactions on Networking (TON)*, 10(4):477–486, 2002.

[68] L. Ying, S. Yang, and R. Srikant. Optimal delay-throughput trade-offs in mobile ad hoc networks. *IEEE Transactions on Information Theory*, 54(9):4119–4143, Sep. 2008.

[69] M. Garetto and E. Giaccone, P. Leonardi. Capacity scaling in ad hoc networks with heterogeneous mobile nodes: The subcritical regime. *IEEE/ACM Transactions on Networking*, 17(6):1888–1901, Dec. 2009.

[70] T. Spyropoulos, K. Psounis, and C. S. Raghavendra. Single-copy routing in intermittently connected mobile networks. In *Sensor and Ad Hoc Communications and Networks, 2004. IEEE SECON 2004. 2004 First Annual IEEE Communications Society Conference on*, pages 235–244. IEEE, 2004.

[71] T. Spyropoulos, K. Psounis, and C. S. Raghavendra. Efficient routing in intermittently connected mobile networks: The multiple-copy case. *IEEE/ACM Transactions on Networking (ToN)*, 16(1):77–90, 2008.

[72] C. Zhang, Y. Fang, and X. Zhu. Throughput-delay tradeoffs in large-scale manets with network coding. In *INFOCOM*, 2010.

[73] C. M. Grinstead and J. L. Snell. *Introduction to Probability, 2nd ed.* American Mathematical Society, 1997.

[74] C. M. Grinstead and J. L. Snell. *Introduction to Probability: Second Revised Edition.* American Mathematical Society, 1997.

[75] Qualnet.

[76] C++ simulator for the packet delivery delay performance in 3D MANETS.

[77] S. Zhou and L. Ying. On delay constrained multicast capacity of large-scale mobile ad-hoc networks. In *INFOCOM*, 2010.

[78] B. Yang, Y. Chen, Y. Cai, and X. Jiang. Packet delivery ratio/cost in MANETs with erasure coding and packet replication. *IEEE Transactions on Vehicular Technology*, 64(5):2062–2070, May. 2015.

[79] C. Hu, X. Wang, and F. Wu. Motioncast: On the capacity and delay tradeoffs. In *MobiHoc*, 2009.

[80] M. J. Neely. *Dynamic power allocation and routing for satellite and wireless networks with time varying channels*. PhD thesis, Massachusetts Institute of Technology, 2003.

[81] E. Altman and F. D. Pellegrini. Forward correction and fountain codes in delay-tolerant networks. *IEEE/ACM Trans. Netw.*, 19(1):1–13, Feb. 2011.

[82] Y. Chen, Y. Shen, X. Jiang, and J. Li. Throughput capacity of ALOHA MANETs. In *ICCC*, 2013.

THIS PAGE INTENTIONALLY LEFT BLANK

Publications

Journal Articles

[1] Wu Wang, Bin Yang, Osamu Takahashi, Xiaohong Jiang, and Shikai Shen. On the Packet Delivery Delay Study for Three-Dimensional Mobile Ad Hoc Networks. *Ad Hoc Networks*, 69: 38–48, February 2018.

Conference Papers

[2] Wu Wang, Bin Yang, Osamu Takahashi, and Xiaohong Jiang. Delivery Delay in 3D MANETs with Packet Redundancy. In *Proc. CANDAR*, 2015.

[3] Wu Wang, Bin Yang, Osamu Takahashi, Xiaohong Jiang, and Shen Shikai. Delivery Probability of 3D MANETs with Packet Replication. In *Proc. NaNA*, 2016.

[4] Wu Wang, Bin Yang, Shen Shikai, Yujian Wang, and Gang Fang. Delay and Capacity in Three-Dimensional Mobile Ad Hoc Networks with Packet Replication. In *Proc. NaNA*, 2017.